Supporting Information

Iron Oxide Surface Chemistry: Effect of Chemical Structure on Binding in Benzoic Acid and Catechol Derivatives

*Katalin V. Korpany, Dorothy D. Majewski, Cindy T. Chiu, Shoronia N. Cross, and Amy Szuchmacher Blum**

Department of Chemistry, McGill University, 801 Sherbrooke Street West, Montreal, QC H3A 0B8, Canada

*Email: amy.blum@mail.mcgill.ca

Additional Experimental Section

Synthesis of 3,5-Dihydroxybenzoic Acid (3,5-DHBA) Functionalized Iron Oxide Nanoparticles (IONP-3,5-DHBA). As synthesized IONP-OA were defrosted to room temperature and redispersed in dry DCM to obtain a 2.50 mg/mL stock solution. 41 mg (0.266 mmol) of 3,5-DHBA (MW = 154.12 g/mol) was weighed in a Teflon capped glass vial and dispersed in 13 mL of dry DCM. 2 mL of stock IONP-OA in DCM (5 mg) was added to the 3,5-DHBA in DCM. 10 µL of 1 M HCl(aq) was added to the reaction mixture. If HCl(aq) was not added to the mixture (no acid added preparation), 10 µL DI water was added instead. Reaction mixture was shaken overnight by vortex at room temperature. After shaking, the reaction mixture was aliquoted in 4 mL aliquots to separate glass vials. Each aliquot of particles was purified by washing with hexane and isopropanol/methanol (1:1) as follows. Particles were magnetically isolated using a handheld neodymium (NdFeB) magnet (3 minutes). Supernatant was removed by pipet. Recovered particle pellets were washed with 3 x 2 mL of hexane, re-isolating particles magnetically and removing wash supernatant by pipet after each wash. Hexane washed particles were subsequently washed with 3 x 2 mL of isopropanol/methanol (1:1) (or 6 x 2 mL isopropanol/methanol (1:1) for samples prepared for FTIR), re-isolating particles magnetically and removing wash supernatant by pipet after each wash.

Synthesis of Dopamine (DA) Functionalized Iron Oxide Nanoparticles (IONP-DA). Synthesis of dopamine-stabilized iron oxide nanoparticles was based on a method reported by

Nagesha et al.[1] As synthesized IONP-OA were defrosted to room temperature and redispersed in dry DCM to obtain a 2.50 mg/mL stock solution. 25 mg (0.132 mmol) of DA·HCl (MW = 189.64 g/mol) was weighed in a Teflon capped glass vial and dispersed in 13 mL of dry DCM. 2 mL of stock IONP-OA in DCM (5 mg) was added to the DA in DCM. 10 µL of 1 M HCl(aq) was added to the reaction mixture. Reaction mixture was shaken overnight by vortex at room temperature. After shaking, the reaction mixture was aliquoted in 2 mL aliquots to separate glass vials. Each aliquot of particles was purified by washing with hexane and methanol as follows. Particles were magnetically isolated using a handheld neodymium (NdFeB) magnet (5 minutes). Light brown, slightly yellow supernatant was removed by pipet. Recovered particle pellets were washed with 3 x 1 mL of hexane, re-isolating particles magnetically and removing clear, colorless wash supernatant by pipet after each wash. Hexane washed particles were subsequently washed with 3 x 1 mL of methanol, re-isolating particles magnetically and removing light tan, clear wash supernatant by pipet after each wash.

Synthesis of 3,4-Dihydroxybenzoic Acid (3,4-DHBA) Functionalized Iron Oxide Nanoparticles (IONP-3,4-DHBA). As synthesized IONP-OA were defrosted to room temperature and redispersed in dry DCM. 41 mg (0.266 mmol) of 3,4-DHBA (MW = 154.12 g/mol) was weighed in a Teflon capped glass vial and dispersed in enough dry DCM to obtain a total reaction volume of 15 mL. 5 mg of stock IONP-OA in DCM was added to the 3,4-DHBA in DCM. 10 µL of 1 M HCl(aq) was added to the reaction mixture. If HCl(aq) was not added to the mixture (no acid added preparation), 10 µL DI water was added instead. Reaction mixture was shaken overnight by vortex at room temperature. After shaking, the reaction mixture was aliquoted in 4 mL aliquots to separate glass vials. Each aliquot of particles was purified by washing with hexane and methanol as follows. Particles were magnetically isolated using a handheld neodymium (NdFeB) magnet (3 minutes). Supernatant was removed by pipet. Recovered particle pellets were washed with 3 x 2 mL of hexane, re-isolating particles magnetically and removing wash supernatant by pipet after each wash. Hexane washed particles were subsequently washed with 3 x 2 mL of methanol, re-isolating particles magnetically and removing wash supernatant by pipet after each wash.

Synthesis of 3,4-Dihydroxyphenylacetic Acid (3,4-DHPA) Functionalized Iron Oxide Nanoparticles (IONP-3,4-DHPA). As synthesized IONP-OA were defrosted to room temperature and redispersed in dry DCM to obtain a 2.50 mg/mL stock solution. 44.5 mg (0.265 mmol) of 3,4-DHPA (MW = 168.15 g/mol) (44.1 mg, 0.262 mmol for nanoparticles prepared for electrokinetic measurements) was weighed in a Teflon capped glass vial and dispersed in 13 mL of dry DCM. 2 mL of stock IONP-OA in DCM (5 mg) was added to the 3,4-DHPA in DCM. 10 µL of 1 M HCl(aq) was added to the reaction mixture. If HCl(aq) was not added to the mixture (no acid added preparation), 10 µL DI water was added instead. Reaction mixture was shaken overnight by vortex at room temperature. After shaking, the reaction mixture was aliquoted in 4 mL aliquots to separate glass vials. Each aliquot of particles was purified by washing with hexane and methanol as follows. Particles were magnetically isolated using a handheld neodymium (NdFeB) magnet (5 minutes, 3 minutes for nanoparticles prepared for electrokinetic measurements). Supernatant was removed by pipet. Recovered particle pellets were washed with 3 x 2 mL of hexane, re-isolating particles magnetically and removing wash supernatant by pipet after each wash. Hexane washed particles were subsequently washed with 3 x 2 mL of methanol, re-isolating particles magnetically and removing wash supernatant by pipet after each wash.

Synthesis of 2,3-Dihydroxybenzoic Acid (2,3-DHBA) Functionalized Iron Oxide Nanoparticles (IONP-2,3-DHBA). As synthesized IONP-OA were defrosted to room temperature and redispersed in dry DCM to obtain a 2.50 mg/mL stock solution. 41 mg (0.266 mmol) of 2,3-DHBA (MW = 154.12 g/mol) was weighed in a Teflon capped glass vial and dispersed in 13 mL of dry DCM. 2 mL of stock IONP-OA in DCM (5 mg) was added to the 2,3-DHBA in DCM. 10 μL of 1 M HCl(aq) was added to the reaction mixture. If HCl(aq) was not added to the mixture (no acid added preparation), 10 μL DI water was added instead. Reaction mixture was shaken overnight by vortex at room temperature. After shaking, the reaction mixture was aliquoted in 4 mL aliquots to separate glass vials. Each aliquot of particles was purified by washing with hexane and methanol (MeOH) as follows. Particles were magnetically isolated using a handheld neodymium (NdFeB) magnet (20 minutes acid preparation, 2–8 minutes no acid preparation). Supernatant was removed by pipet. Recovered particle pellets were washed with 3 x 2 mL of hexane, re-isolating particles magnetically and removing wash supernatant by pipet after each wash. Hexane washed particles were subsequently washed with 3 x 2 mL of MeOH (or 4 x 2 mL MeOH for the HCl preparation characterized by FTIR), re-isolating particles magnetically and removing wash supernatant by pipet after each wash. Hexane wash supernatants were clear and colorless, in contrast to the MeOH washes that were an intense indigo (HCl added preparation) or a light indigo color (DI water added preparation).

Synthesis of 2,5-Dihydroxybenzoic Acid (2,5-DHBA) Functionalized Iron Oxide Nanoparticles (IONP-2,5-DHBA). As synthesized IONP-OA were defrosted to room temperature and redispersed in dry DCM. 41 mg (0.266 mmol) of 2,5-DHBA (MW = 154.12 g/mol) was weighed in a Teflon capped glass vial and dispersed in dry DCM to obtain a total reaction volume of 15 mL. 5 mg of stock IONP-OA in DCM was added to the 2,5-DHBA in DCM. 10 μL of 1 M HCl(aq) was added to the reaction mixture. If HCl(aq) was not added to the mixture (no acid added preparation), 10 μL DI water was added instead. Reaction mixture was shaken overnight by vortex at room temperature. After shaking, the reaction mixture was aliquoted in 4 mL aliquots to separate glass vials. Each aliquot of particles was purified by washing with hexane and methanol (MeOH) as follows. Particles were magnetically isolated using a handheld neodymium (NdFeB) magnet (5 minutes). Supernatant was removed by pipet. Recovered particle pellets were washed with 3 x 2 mL of hexane, re-isolating particles magnetically and removing wash supernatant by pipet after each wash. Hexane washed particles were subsequently washed with 3 x 2 mL of MeOH, re-isolating particles magnetically and removing wash supernatant by pipet after each wash. MeOH supernatants were clear and green-blue in color for the HCl(aq) added preparation, but clear and colorless in the DI water added case.

Synthesis of Salicylic Acid (SA) Functionalized Iron Oxide Nanoparticles (IONP-SA). As synthesized IONP-OA were defrosted to room temperature and redispersed in dry DCM to obtain a 2.50 mg/mL stock solution. 37.5 mg (0.272 mmol) of SA (MW = 138.12 g/mol) was weighed in a Teflon capped glass vial and dispersed in 13 mL of dry DCM. 2 mL of stock IONP-OA in DCM (5 mg) was added to the SA in DCM. 10 μL of 1 M HCl(aq) was added to the reaction mixture. If HCl(aq) was not added to the mixture (no acid added preparation), 10 μL DI water was added instead. Reaction mixture was shaken overnight by vortex at room temperature. After shaking, the reaction mixture was aliquoted in 4 mL aliquots to separate glass vials. Each aliquot of particles was purified by washing with hexane and methanol (MeOH) as follows. Particles could not be magnetically isolated using a handheld neodymium (NdFeB) magnet,

therefore DCM was evaporated under N_2(g) flow. Recovered particles were washed with 3 x 2 mL of hexane, re-isolating particles magnetically and removing wash supernatant by pipet after each wash. Hexane washed particles were subsequently washed with 3 x 2 mL of MeOH, re-isolating particles magnetically and removing wash supernatant by pipet after each wash. Hexane wash supernatants were clear and colorless, in contrast to the MeOH washes that were medium purple-violet in color (HCl added preparation) or a pale orange-pink (DI water added preparation).

Synthesis of 2,4-Dihydroxybenzoic Acid (2,4-DHBA) Functionalized Iron Oxide Nanoparticles (IONP-2,4-DHBA). As synthesized IONP-OA were defrosted to room temperature and redispersed in dry DCM to obtain a 2.50 mg/mL stock solution. 41 mg (0.266 mmol) of 2,4-DHBA (MW = 154.12 g/mol) was weighed in a Teflon capped glass vial and dispersed in 13 mL of dry DCM. 2 mL of stock IONP-OA in DCM (5 mg) was added to the 2,4-DHBA in DCM. 10 µL of 1 M HCl(aq) was added to the reaction mixture. If HCl(aq) was not added to the mixture (no acid added preparation), 10 µL DI water was added instead. Reaction mixture was shaken overnight by vortex at room temperature. After shaking, the reaction mixture was aliquoted in 4 mL aliquots to separate glass vials. Each aliquot of particles was purified by washing with hexane and acetone as follows. Particles were magnetically isolated using a handheld neodymium (NdFeB) magnet (3 minutes). Supernatant was removed by pipet. Recovered particle pellets were washed with 3 x 2 mL of hexane, re-isolating particles magnetically and removing wash supernatant by pipet after each wash. Hexane washed particles were subsequently washed with 3 x 2 mL acetone, re-isolating particles magnetically and removing wash supernatant by pipet after each wash. Using acquired FTIR spectra as a guide, washing with 6 x 2 mL of acetone was required to obtain nanoparticles that were completely free of excess ligand. Acetone wash supernatants were clear and a light tan-orange in color for the HCl(aq) added preparation, but clear and colorless in the DI water added case.

Synthesis of 2,6-Dihydroxybenzoic Acid (2,6-DHBA) Functionalized Iron Oxide Nanoparticles (IONP-2,6-DHBA). As synthesized IONP-OA were defrosted to room temperature and redispersed in dry DCM to obtain a 1.25 mg/mL stock solution. 41 mg (0.266 mmol) of 2,6-DHBA (MW = 154.12 g/mol) was weighed in a Teflon capped glass vial and dispersed in 11 mL of dry DCM. 4 mL of stock IONP-OA in DCM (5 mg) was added to the 2,5-DHBA in DCM. 10 µL of 1 M HCl(aq) was added to the reaction mixture. If HCl(aq) was not added to the mixture (no acid added preparation), 10 µL DI water was added instead. Reaction mixture was shaken overnight by vortex at room temperature. After shaking, the reaction mixture was aliquoted in 2 mL aliquots to separate glass vials. Each aliquot of particles was purified by washing with hexane and methanol as follows. Particles were magnetically isolated using a handheld neodymium (NdFeB) magnet (3 minutes). Supernatant was removed by pipet. Recovered particle pellets were washed with 3 x 1 mL of hexane, re-isolating particles magnetically and removing the clear, colorless wash supernatant by pipet after each wash. Hexane washed particles were subsequently washed with 3 x 1 mL of methanol, re-isolating particles magnetically and removing indigo or light blue-violet wash supernatant (HCl and DI water preparations, respectively) by pipet after each wash.

Further Purification of IONP-3,5-DHBA DI Water Washed Samples Prepared for FTIR. After initial spectra were acquired, the remaining nanoparticles were subject to further purification as follows. Any remaining isopropanol/methanol was removed under N_2(g) flow and

2 mL of DI water was added to the dried nanoparticles. Nanoparticles were sonicated briefly to delaminate and recollected magnetically for 2 minutes, then the wash supernatant removed by pipet. Particles were washed with an additional 2 x 2 mL of fresh DI water, removing the wash supernatant by pipet after each 2 mL portion. The recovered nanoparticles were rinsed with 1 mL of isopropanol, to help remove excess water, and 20 μL of methanol was added to the nanoparticles in order to create a nanoparticle slurry for drop-casting (for FTIR spectra acquisition).

Further Purification of IONP-3,4-DHPA Samples Prepared for FTIR ("2x washed" samples). The IONP-3,4-DHPA (HCl added) sample prepared for FTIR was subject to further purification after initial IR spectra were obtained. IONP-3,4-DHPA (HCl added) was re-dispersed in 100 μL of methanol for preparation of nanoparticle films for FTIR analysis. After initial FTIR spectra were acquired, the solvent was removed from the nanoparticles under nitrogen flow. 0.5 mL of acetone was added to the brown residue and the resulting cloudy black-brown mixture was vortexed and sonicated for 10 pulses using a bath sonicator. The mixture was subsequently removed to a 1.5 mL Eppendorf tube and centrifuged at 6,500 rpm (4,105 × g) (Sorvall PICO, Thermo Fisher Scientific (Waltham, MA, USA)) at room temperature (RT) for 10 minutes to pellet the nanoparticles. After 10 minutes, a very light tan-colorless, clear supernatant was removed by pipet from a hard dark brown-black pellet. The pellet was resuspended in 0.5 mL of fresh acetone, vortexed to resuspend to result in a dark brown-black mixture, then centrifuged for 10 minutes to re-pellet (6,500 rpm, RT). After centrifugation, a clear, colorless supernatant was removed by pipet. The pellet was redispersed in 50 μL of fresh acetone, by brief vortexing and sonication to result in a dark brown-black mixture. FTIR spectra of the further purified nanoparticles was then acquired as previously described. Further purification of IONP-3,4-DHPA (DI water), and subsequent spectra acquisition, was performed in the same way as for IONP-3,4-DHPA (HCl), except the initial solvent was not removed under nitrogen flow and 0.5 mL acetone was added directly to the remaining nanoparticle solution (after initial FTIR spectra were obtained).

Electrokinetic Measurements. Nanoparticles used for electrokinetic measurements were prepared as previously stated in the detailed nanoparticle syntheses (Supporting Information) with some modifications as outlined in Table S13. Purified nanoparticles were resuspended in filtered (0.2 μm syringe filter; Whatman) 0.2 M Tris buffer pH 9.21 with brief sonication (10, 1 second pulses). IONP-3,4-DHPA resuspension was allowed to sit for 90 minutes before further processing. The prepared IONP-3,4-DHPA solution was magnetically separated using a rare-Earth (NdFeB) magnet for 1 minute, to remove any unsuspended particles, and the supernatant used for electrokinetic measurements. Nanoparticle solutions were diluted with 0.2 M Tris buffer pH 9.21 to a concentration of 0.20 mg/mL (as Fe_3O_4) for measurement. Nanoparticle concentrations were determined in as outlined in the section below, "Iron Oxide Nanoparticle (IONP) Concentration Determination" (Supporting Information).

Electrokinetic measurements were performed on a ZetaPlus zeta potential analyzer (Brookhaven Instruments Corporation, Holtsville, NY, USA) at 25 °C, collecting 10 measurements, obtained over 3 cycles, for each sample. Values for electrophoretic mobility and zeta potential (using the Smoluchowski approximation) were determined using the accompanying Zeta Analysis software (Brookhaven Instruments Corporation, Holtsville, NY, USA). Reported values for zeta potential and mobility are an average of 10 measurements.

Iron Oxide Nanoparticle (IONP) Concentration Determination. IONP concentration was determined as outlined in Korpany et al.[2] with minor modifications as follows. Briefly, a 0.100 mL aliquot of purified IONP solution in buffer was collected, to which 0.100 mL of 37% HCl was added. The solution was incubated at ~70 °C for 10 minutes to fully digest IONPs, followed by dilution with 0.300 mL of DI water. Two 0.100 mL aliquots of the digested solution were collected, to which 0.100 mL of 0.1 M H_2O_2(aq) was added and the solutions incubated at room temperature for 10 minutes, in order to oxidize all iron to Fe^{3+}. After 10 minutes, 0.200 mL of 0.25 M Tiron(aq) (4,5-dihydroxy-1,3-benzenedisulfonic acid) was added to the solutions, followed by 0.350 mL of 0.2 M Tris buffer (pH 9.21), yielding blue-green solutions. The solutions were then converted to a red-orange color by the addition of 80.0 μL of 4 M KOH(aq). The solutions were incubated at room temperature for 15 minutes in order to allow the color to fully develop prior to UV–visible (UV–vis) absorbance measurements. UV–vis measurements were performed from 800–400 nm (Cary 100 Bio spectrophotometer, Agilent Technologies Inc., Santa Clara, CA, USA; 0.3 cm pathlength quartz cuvette), and the absorbance at 480 nm used to quantify the total iron present ($\varepsilon(Fe^{3+}, 480nm) = 109.5\ (mg/mL)^{-1}\ cm^{-1}$).

Nanoparticle UV–Visible Spectroscopy. All nanoparticle UV–visible (UV–vis) spectra were acquired using a Cary 100 Bio spectrophotometer (Agilent Technologies Inc., Santa Clara, CA, USA) from 800–200 nm using a 0.3 cm pathlength quartz cuvette. Purification of the ligand exchange mixture was performed as previously stated in the in the detailed nanoparticle syntheses (Supporting Information) with modifications as outlined in Table S13. Purified nanoparticles were resuspended in buffer as outlined in Table S13. For each nanoparticle resuspension, any undispersed nanoparticles were magnetically separated by application of a handheld neodymium (NdFeB) to the sample vial for 5 minutes and the supernatant used for UV–vis spectroscopy.

Preparation of Fe(II) and Fe(III) 2,6-DHBA Complexes and UV–Visible Spectroscopy of Complexes and Ligand Exchange Reaction Supernatants. All UV–visible (UV–vis) spectra were acquired using a Cary 100 Bio spectrophotometer (Agilent Technologies Inc., Santa Clara, CA, USA) from 800–200 nm. The spectrum of the ligand exchange supernatants were obtained, at their original concentrations, from retained methanol wash supernatants (originating from the purification of ligand-nanoparticle reaction mixture) using a 0.3 cm pathlength quartz cuvette. Purification of ligand exchange mixture was performed as previously stated in the detailed nanoparticle syntheses (Supporting Information).

Solutions of 1 mM Fe(II) and Fe(III) were prepared by dissolving $FeCl_2 \cdot 4H_2O$ and $FeCl_3 \cdot 6H_2O$, respectively, in an appropriate amount of 0.1 M HCl(aq). 2,6-DHBA was dissolved in methanol (MeOH) to prepare a 6 mM solution. To prepare iron-ligand complexes for UV–vis spectroscopy, equivalent volumes of 6 mM 2,6-DHBA in MeOH and previously prepared 1 mM Fe(II) or Fe(III) solutions were combined. A ligand control sample was also prepared by mixing 0.6 mL of 6 mM 2,6-DHBA in MeOH and 0.6 mL of 0.1 M HCl(aq) in a 1.5 mL Eppendorf tube. UV–vis spectra of complexes and control were acquired without dilution using a 1 cm pathlength cuvette against a 1:1 (MeOH/0.1 M HCl(aq)) baseline.

Additional Tables and Figures

Table S1. Summary of Nanoparticle Diameter and TEM Sample Plating Conditions for IONP-OA and Ligand Exchanged IONPs

Nanoparticle	Additive	Mean nanoparticle diameter (nm)	Median nanoparticle diameter	*N*	Solvent used for TEM sample preparation[a]
IONP-OA (Batch 1)	N/A	5.0 ± 0.8	5.0	2061	hexane
(Batch 2)	N/A	5.4 ± 0.9	5.3	3805	hexane
IONP-3,5-DHBA[b]	HCl	5.5 ± 0.9	5.5	5425	DMSO
	DI water	5.4 ± 0.9	5.3	4784	DMSO
IONP-DA[b]	HCl	5.6 ± 0.9	5.5	5895	20 mM sodium acetate buffer pH 5.00
IONP-3,4-DHBA	DI water	5.0 ± 0.7	5.0	154	0.2 M Tris buffer pH 9.26
IONP-3,4-DHPA	HCl	5.5 ± 0.8	5.4	487	0.2 M Tris buffer pH 9.26
	HCl	5.4 ± 0.9[b]	5.3	2323	0.2 M Tris buffer pH 9.26
	DI water	5.1 ± 0.8[b]	5.0	4916	0.2 M Tris buffer pH 9.26
IONP-2,3-DHBA	HCl	5.1 ± 0.8	5.0	2564	DMF
	DI water	5.3 ± 0.9	5.2	66	20 mM sodium phosphate buffer pH 7.19
IONP-2,5-DHBA	HCl	5.2 ± 0.8	5.1	5198	DMF
	DI water	5.3 ± 0.8	5.1	2378	DMF
IONP-SA	HCl	5.2 ± 0.8	5.1	5373	DMSO
	DI water	5.1 ± 0.8	5.0	2773	DMSO
IONP-2,4-DHBA[b]	HCl	5.2 ± 0.9	5.1	2836	DMSO
	DI water	5.3 ± 0.8	5.1	4163	DMSO
IONP-2,6-DHBA[b]	DI water	5.4 ± 0.9	5.2	4051	DMSO

[a]Prior to sample plating, nanoparticle solutions were briefly vortexed and sonicated for 10, 1 second pulses each to ensure full redispersal.
[b]Ligand exchanged nanoparticles produced using IONP-OA Batch 2.
Key: N/A, not applicable.

Table S2. Modified Nanoparticle Purification Parameters for Some TEM Samples[a]

Nanoparticle TEM Samples	Reaction additive	Reaction mixture volume (mL)	1st wash	2nd wash
IONP-3,5-DHBA	HCl	2	3 x 1 mL hexane	3 x 1 mL methanol
IONP-3,4-DHPA	HCl	3	3 x 2 mL hexane	3 x 2 mL methanol
	HCl[b]	2	3 x 1 mL hexane	3 x 1 mL methanol
	DI water[b]	2	3 x 1 mL hexane	3 x 1 mL methanol
IONP-2,5-DHBA	HCl	2.8	3 x 2 mL hexane	3 x 2 mL methanol
IONP-2,4-DHBA	HCl	2	3 x 1 mL hexane	3 x 1 mL methanol
	DI water	2	3 x 1 mL hexane	3 x 1 mL acetone

[a]In all other cases, nanoparticle purifications for TEM samples were conducted as outlined in the "Additional Experimental Section".
[b]Nanoparticles synthesized with IONP-OA Batch 2.

Table S3. Modified Nanoparticle Purification Parameters for Some Solubility Determinations[a]

Nanoparticle	Reaction additive	Solubility determination	Reaction mixture volume (mL)	1st wash	2nd wash
IONP-3,5-DHBA	HCl	DMSO	2	3 x 1 mL hexane	3 x 1 mL methanol or 6 x 1 mL isopropanol/methanol (1:1)
		DMF	2	3 x 1 mL hexane	1 x 1 mL ethanol then 2 x 1 mL acetone
	DI water	DI water	2	3 x 1 mL hexane	3 x 1 mL methanol
IONP-2,3-DHBA	HCl	DMSO	4	3 x 2 mL hexane	4 x 2 mL methanol
IONP-2,4-DHBA	HCl	DMSO	2	3 x 1 mL hexane	3 x 1 mL methanol
			4	3 x 2 mL hexane	6 x 2 mL acetone

[a]In all other cases, nanoparticle purifications for solubility determinations were conducted as outlined in the "Additional Experimental Section".

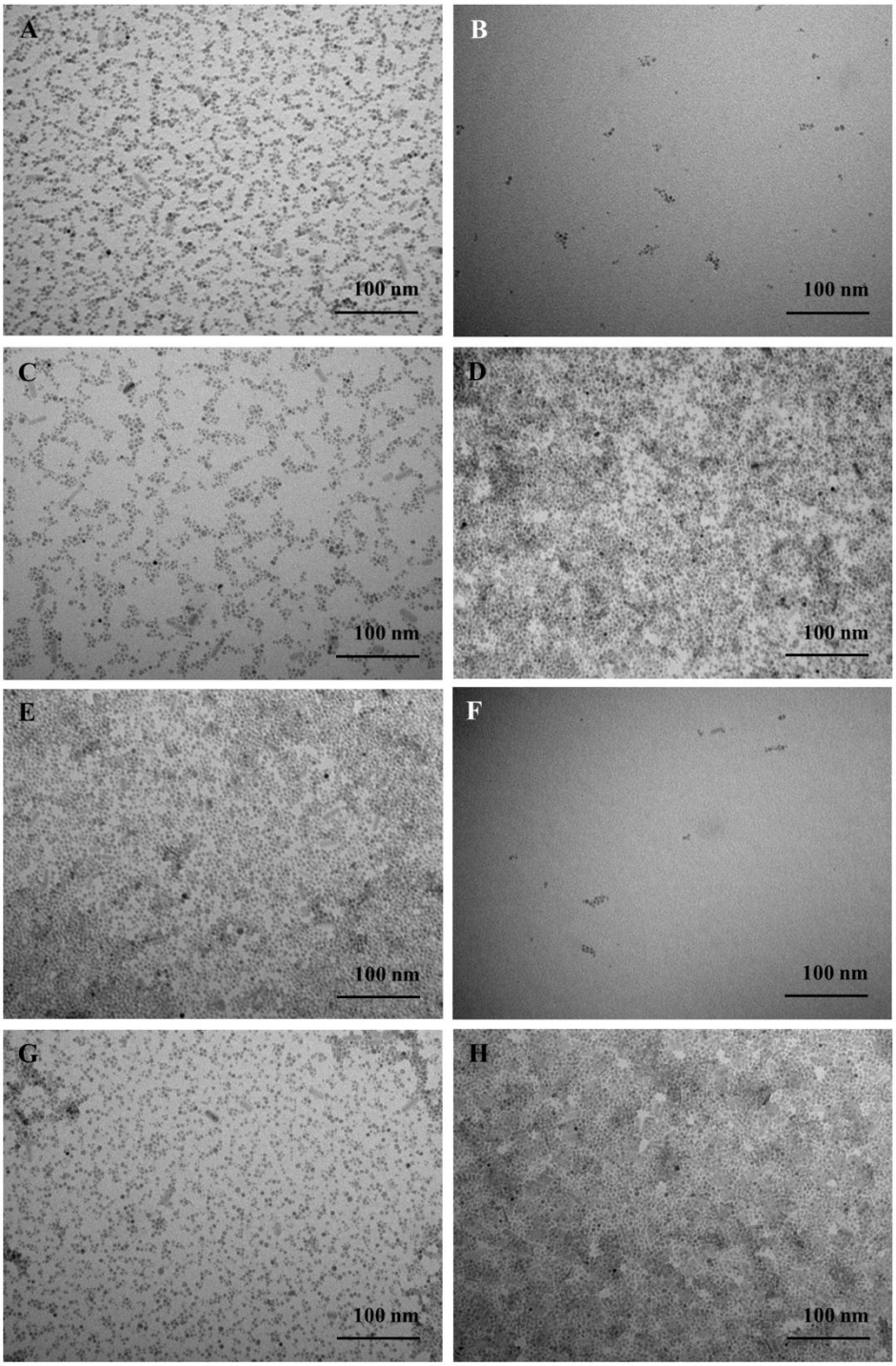

Figure S1. TEM images of (A) IONP-OA (Batch 1). The following ligand exchanged nanoparticles were synthesized using Batch 1 IONP-OA with HCl unless otherwise specified: (B) IONP-3,4-DHBA (DI water), (C) IONP-2,5-DHBA, (D) IONP-2,5-DHBA (DI water), (E) IONP-2,3-DHBA, (F) IONP-2,3-DHBA (DI water), (G) IONP-SA, and (H) IONP-SA (DI water).

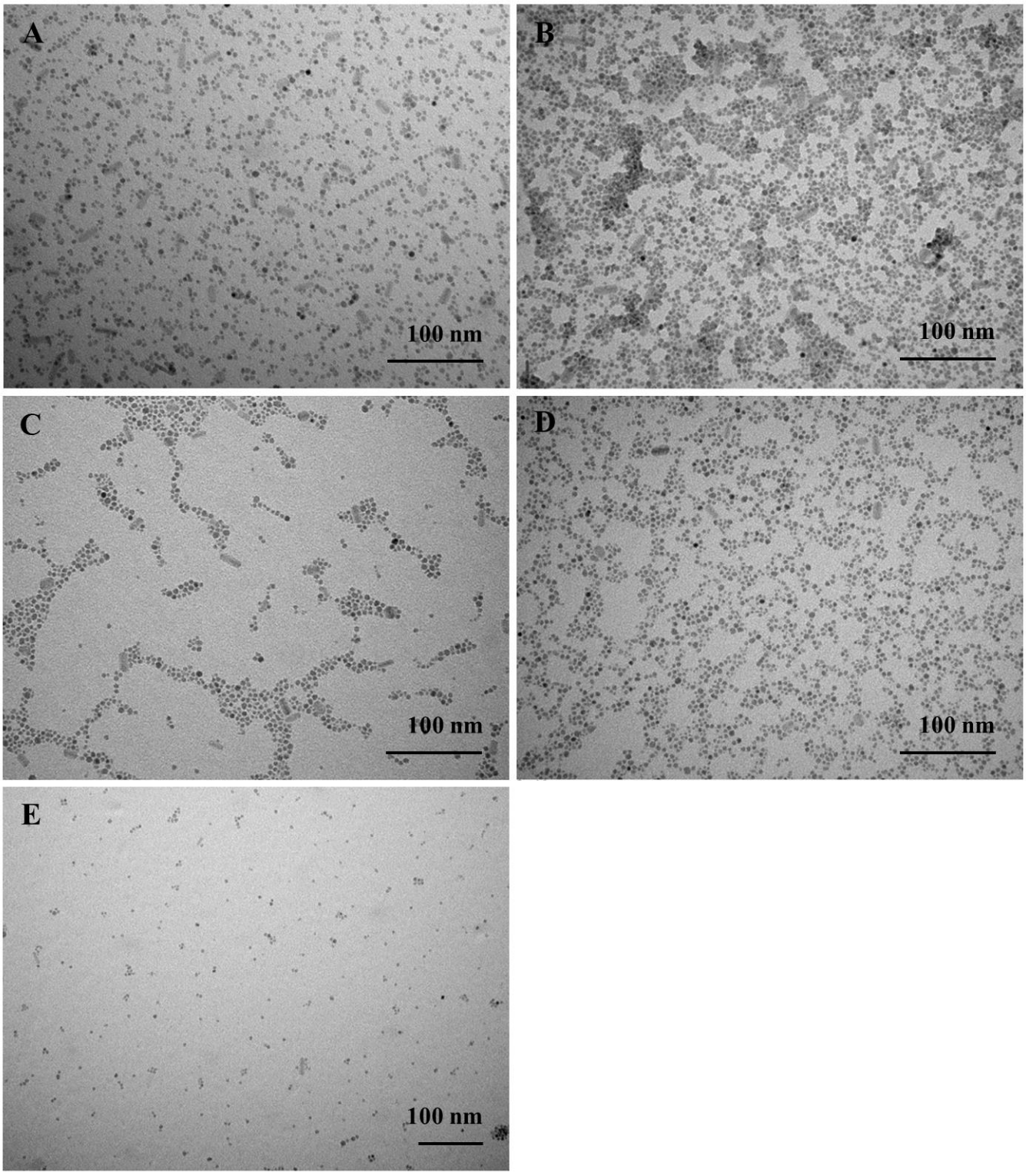

Figure S2. TEM images of (A) IONP-OA (Batch 2), (B) IONP-DA (Batch 2), (C) IONP-3,4-DHPA (Batch 2), (D) IONP-3,4-DHPA (Batch 2, DI water), and (E) IONP-3,4-DHPA (Batch 1). Ligand exchanged nanoparticles were prepared from IONP-OA from either Batch 1 or 2 as noted with HCl added to the ligand exchange mixture, unless otherwise specified.

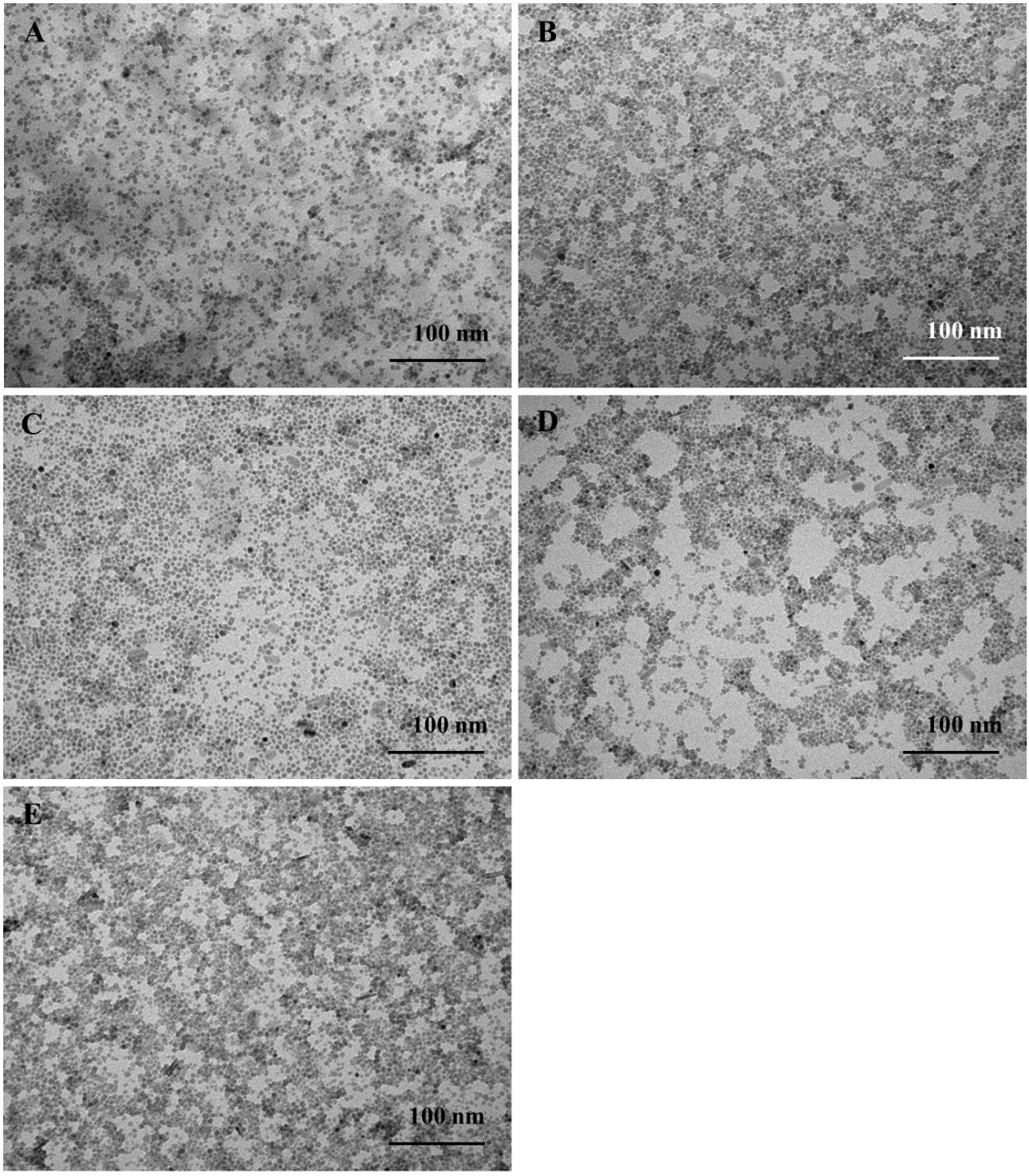

Figure S3. TEM images of (A) IONP-3,5-DHBA, (B) IONP-3,5-DHBA (DI water), (C) IONP-2,4-DHBA, (D) IONP-2,4-DHBA (DI water), and (E) IONP-2,6-DHBA (DI water) prepared from IONP-OA (Batch 2) with HCl, unless otherwise specified.

FTIR Band Assignments for IONP-OA, Ligand Exchanged Nanoparticles, Investigated Ligands, and Ligand Sodium Salts

Insights regarding all assignments listed in this section are provided by the references indicated as well as by Larkin[3] and Lambert et al.[4] Assignments for the ν(Fe–O) mode for nanoparticle samples were based on literature data for bulk magnetite (Fe_3O_4)[5] and for other Fe_3O_4 nanoparticles.[6]

Table S4. Observed Bands (cm^{-1}) and Tentative Assignments from 4000–400 cm^{-1} for Oleic Acid (OA), Sodium Oleate, and IONP-OA

Oleic acid (OA)	Sodium oleate	IONP-OA (Batch 1)	IONP-OA (Batch 2)	Tentative assignments
~3300–2400br	not visible	3378br	3152br	ν(O–H)
3005[7]	3007[8]	3006	3004	ν(=C–H) (vinyl)[9]
~2955sh	2956[8]	2954	2954	$\nu_{as}(CH_3)$[9c]
2922[7a, 7b]	2919[8]	2923	2920	$\nu_{as}(CH_2)$[9a, 9c, 10]
not visible	2874[8]	not visible	not visible	$\nu_s(CH_3)$
2853[7a, 7b]	2850[8]	2858	2851	$\nu_s(CH_2)$[9a, 9c, 10, 11]
1708[7b, 7c, 8, 9b, 9c]	not present	not present	not present	ν(C=O)[9a, 10a, 12]
N/A	1559[8]	1520	1519	$\nu_{as}(COO^-)$
1464	1462	not visible	not visible	$\beta_s(CH_2)$[9c] (scissor) or β(C–OH)[7b, 9a, 10a]
N/A	1444[8] or 1424	1428[9b]	1425[9b]	$\nu_s(COO^-)$
1412	not visible	~1412sh	1411	β_{as}(=C–H) (rock) or CH_3 umbrella mode[7b]
1377	1379	~1379sh	~1379sh	$\delta_s(CH_3)$[9c]
1284[7b]	1278w	1262w	1261w	ν(C–O) (O=C–OH)[10a]
935	923	not present	not present	γ(C=C)[9c] or γ(C–OH)[3, 7b, 10a] (wag)
722[3, 7a, 7b]	721	not visible	not visible	β_{as} (CH_2) (rock)[9c]
N/A	N/A	591	580	ν(Fe–O)

Key:

br, broad; sh, shoulder; w, weak.
ν, stretch; β, in-plane bend; δ, bend, with no defined plane of motion; γ, out-of-plane bend.
as, asymmetric; s, symmetric.
not visible: A given band was not visible but may be part of a larger broad absorption in the area. The band may exist but this cannot be confirmed or denied.
not present: A given band was not visible and is unlikely to be part of a larger broad overlapping absorption.
N/A: not applicable.

Table S5. Observed Bands (cm^{-1}) and Tentative Assignments from 4000–400 cm^{-1} for 3,5-Dihydroxybenzoic Acid (3,5-DHBA) and IONP-3,5-DHBA

3,5-DHBA	IONP-3,5-DHBA			Tentative assignments
	(HCl)	(DI water)	(DI water, water washed)	
3199br[13]	3202br	3306br	3159br	ν(O–H)
N/A	2930w	2929w	not visible	$\nu_{as}(CH_2)$
N/A	not visible	2858w	not present	$\nu_{s}(CH_2)$
1682[13]	1693	1694	not present	ν(C=O), $\nu(CC)_{ar}$ (8a)[a]
1606[b, 13]	**1600**	**1603**	**1605**	**$\nu(CC)_{ar}$ (8b)[14]**
N/A	1584sh	~1552sh	1523[c]	$\nu_{as}(COO^-)$
1514[13]	1517	1518	1523[c]	$\nu(CC)_{ar}$ (19b)
1479[13]	1485	not visible	not visible	$\nu(CC)_{ar}$, β(C–OH)
1415[13]	1410	1412	not visible	β(C–OH)[15]
N/A	not visible	not visible	1396	$\nu_{s}(COO^-)$
1328	1337	1333	not visible	β(C–OH) (Ar–OH)
1300[13]	**1303**	**1304**	**1302**	**ν(C–H) (13)[14]**
1260[13]	1267	not visible	not visible	ν(C–O) (O=C–OH), $\nu(CC)_{ar}$
1199	1204	1208	1209	ν(C–O) (Ar–OH)[16]
1159[13]	**1159**	**1160**	**1158**	**β(C–H) (9b)**
1106[13]	1109sh	~1114sh	not visible	β(C–H) (18a) (translation)[14]
1005	**1002**	**1004**	**1005**	**α(CCC) (12) (radial skeletal, trigonal symmetry)[14] or 1,3,5 radial in phase stretch,[3] mix of ring stretch and bending[15]**
939	944	~937sh	not visible	γ(C–OH) (O=C–OH dimer, wag)[3, 15] or ν(C–H) (7b)[14]
916	not visible	not present	not present	γ(C–H)[13] or γ(C–OH) (O=C–OH dimer, wag)[3, 15]
869[13]	867	858	not visible	γ(C–H) (17b)[14]

851	not visible	858	not visible	γ(C–H) (lone H wag, 1,3,5 substitution)[3]
697	697w	~695sh	not visible	ring pucker[3, 15]
677w	not visible	not visible	not visible	ϕ(CCC) (4)[13] (skeletal)[14], ring pucker[3, 15]
663[13]	663	669sh	not visible	α(CCC) (1) (radial skeletal)
617[13]	not visible	not visible	not visible	ϕ(CC) (ring pucker)
N/A	580	582	572	*ν*(Fe–O)
593[13]	not visible	not visible	not visible	α(CCC)
562[13]	557	not visible	not visible	γ(O–H)
532[13]	527	not visible	not visible	α(CCC) (6a) (skeletal)[14]
467[13]	468	not visible	not visible	α(CCC) (6b) (skeletal)[14]

[a]Numbers in brackets correspond to vibrational modes outlined in Láng and Varsányi.[14]
[b]Vibrations in bold are associated with the aromatic ring of 3,5-DHBA.
[c]Band observed at 1523 cm^{-1} is likely a result of a combination of $\nu_{as}(COO^-)$ + $\nu(CC)_{ar}$ (19b).

Key:
br, broad; sh, shoulder; w, weak.
ν, stretch; β, in-plane bend; α, aromatic in-plane deformation; γ, out-of-plane bend; ϕ, aromatic out-of-plane deformation.
as, asymmetric; s, symmetric.
ar: aromatic ring.
not visible: A given band was not visible but may be part of a larger broad absorption in the area. The band may exist but this cannot be confirmed or denied.
not present: A given band was not visible and is unlikely to be part of a larger broad overlapping absorption.
N/A: not applicable.

Table S6. Observed Bands (cm^{-1}) and Tentative Assignments from 4000–400 cm^{-1} for Dopamine (DA) and IONP-DA

Dopamine (DA)	IONP-DA (HCl)	Tentative assignments
3339br	3213br	ν(O–H),[17] ν(N–H_2)
3039[17a]	not visible	ν(C–H)$_{ar}$
2929	2927	ν_{as}(CH_2)
not visible	2858	ν_s(CH_2)
1600[17a]	1605	δ_s(NH_2) (scissor)[15, 18]
1617,[17a] 1584,[17] 1499,[17b, 19]	1485[19]	ν(CC)$_{ar}$
not visible	1485	ν(C–O) (semiquinone)[19, 20]
1471	not present	β_s(CH_2) (scissor)[17a] or ν(CC)$_{ar}$[17b, 21]
N/A	1427w	ν(COO^-)$_{as}$ (incomplete removal of OA)
1393[21]	not present	β(C–O–H) (Ar–OH)
1343[17a]	1354	γ_s(CH_2) (wag)
1321[17b]	not present	β(C–O–H) (Ar–OH)
1285[17a]	not visible or 1267	ν(C–O) (Ar–OH)[19]
1261	1267	γ_{as}(CH_2) (twist)[17a] or β(C–C–N)
1206	1222w	β(C–C–N)[4]
1190, 1175	~1202sh, w	ν(C–C) + ν(C–O) (Ar–OH)[17, 21]
1146	1150	β(C–H)$_{ar}$
1114[21]	1121	β(C–H)$_{ar}$
1081	1088w	ν(C–C–N)[3, 4, 15]
1014[17a]	1012	ν(C–N)
963[17a]	972	β_{as} (CH_2) (rock)
876,[17a, 21] 814[21]	882	γ(C–H)$_{ar}$ (lone H wag, 1,3,4 substitution)[3, 4]
791	803	γ(N–H) (wag)[4] or γ(C–H)$_{ar}$[17a, 21] (2

		adjacent H wag, 1,3,4 substitution)[3]
773	not present	β_{as} (CH_2) (rock)[17a] or γ(C–N–H)[21]
751[21]	not visible	$\gamma(CCC)_{ar}$
725w[17a]	not visible	$\delta(CCC)_{ar}$[17b] or β_{as} (CH_2) (rock)
598[17b, 21]	not visible	$\delta(CCC)_{ar}$
N/A	582	*ν*(Fe–O)
558sh[17b, 21], 539	not visible	δ(CCO)
475[17a]	not visible	$\delta(CCC)_{ar}$[21] or δ(CCC–O)[17b]
460	not visible	$\delta(CCC)_{ar}$[21] or γ(CCC–O)[17]

Key:

br: broad.

ν, stretch; δ, bend, with no defined plane of motion; β, in-plane bend; γ, out-of-plane bend; α, aromatic in-plane deformation; ϕ, aromatic out-of-plane deformation.

as, asymmetric; s, symmetric.

not visible: A given band was not visible but may be part of a larger broad absorption in the area. The band may exist but this cannot be confirmed or denied.

not present: A given band was not visible and is unlikely part of a larger broad overlapping absorption.

N/A: not applicable.

Table S7. Observed Bands (cm^{-1}) and Tentative Assignments from 4000–400 cm^{-1} for 3,4-Dihydroxybenzoic Acid (3,4-DHBA), the Sodium Salt of 3,4-DHBA (Na-3,4-DHB), and IONP-3,4-DHBA

3,4-DHBA	Na-3,4-DHB	IONP-3,4-DHBA (DI water)	Tentative assignments
3320br, 2534	3305br	3168br	ν(O–H)
N/A	N/A	2925	$\nu_{as}(CH_2)$
N/A	N/A	2855	$\nu_{s}(CH_2)$
1654	1679w[22]	1654	ν(C=O) (dimer)
1597[23]	1613	1603	$\nu(CC)_{ar}$[22, 24] (8b)[a, 14]
1527[23]	1518	not visible	$\nu(CC)_{ar}$[24b] (19b)[14]
N/A	1541[22, 24b]	1582[b]	$\nu_{as}(COO^-)$
not present	~1490sh	1491	$\nu(CC)_{ar}$[22, 25] or ν(C–O) (semiquinone)[20]
1421[23, 24b]	1426[22]	1432sh	$\nu(CC)_{ar}$ (19a)[14]
1392,[14, 23] 1364	1350	1388	β(C–OH) (O=C–OH or Ar–OH)
N/A	1380	1388	$\nu_{s}(COO^-)$
~1307sh,[14] 1278	1278	1276	ν(C–O) (O=C–OH)[23] + ν(C–H) (7a)[14]
1244sh,[22, 23, 24b] 1221	1242,[22] 1208	not visible	ν(C–O) (Ar–OH)[15, 16]
1155	not visible	not visible	β(C–H)[16] (18a) (translation)[14]
1120	1132	1124	ν(C–H) (13)[14] or β(C–H)[16, 22–24]
1094	1094	1100	β(C–H)[16, 23, 24b] (18b) (translation)[14]
942	950	949	ν(C–H) (7b)[14]
942 or 910	950	949	γ(C–OH) (O=C–OH dimer, wag)[3, 15]
880	879	886	γ(C–H) (5)[14] or lone H wag (1,3,4 substitution)[3, 4]
831	834w	not visible	γ(C–H) (11)[14] (1,3,4 substitution)[4]
764	773	774	α(CCC) (12) (radial skeletal)[14] or 2

			adjacent H wag (1,3,4 substitution)[3]
727w	not visible	not visible	α(CCC) (1) (radial skeletal)[14]
642	647	not visible	γ(C=O)[14]
599	609	not visible	γ(O–H)[14]
N/A	N/A	572	*ν*(Fe–O)
556	547	not visible	α(CCC) (6a) (radial skeletal) or ϕ(CCC) (16a) (skeletal)[14]
546	547	not visible	α(CCC) (6a) (radial skeletal)[14]
not visible	461	not visible	α(CCC) (6b) (skeletal)[14]

[a]Numbers in brackets correspond to vibrational modes outlined in Láng and Varsányi.[14]
[b]Band may alternatively be a ring vibration.

Key:
br, broad; sh, shoulder; w, weak.
ν, stretch; β, in-plane bend; γ, out-of-plane bend; α, aromatic in-plane deformation; ϕ, aromatic out-of-plane deformation.
as, asymmetric; s, symmetric.
not visible: A given band was not visible but may be part of a larger broad absorption in the area. The band may exist but this cannot be confirmed or denied.
N/A: not applicable.

Table S8. Observed Bands (cm^{-1}) and Tentative Assignments from 4000–400 cm^{-1} for 3,4-Dihydroxyphenylacetic Acid (3,4-DHPA), the Sodium Salt of 3,4-DHPA (Na-3,4-DHP), and IONP-3,4-DHPA

3,4-DHPA	Na-3,4-DHPA	IONP-3,4-DHPA				Tentative assignments
		(HCl)	(HCl) (2x washed)	(DI water)	(DI water) (2x washed)	
~3475–2400br	3658, 3032br	3405br	3188br	3165br	3180br	ν(O–H)
2943	2943	not visible	not visible	not visible	2926w	$\nu_{as}(CH_2)$
2843w	2830	not visible	not visible	not visible	not visible	$\nu_{s}(CH_2)$
1682	not present	1694	1700	1702	1702	ν(C=O)
1610, 1514, 1466	1603, 1522, 1458	1604, 1520,	1591, 1524	1590, 1523	1524	$\nu(CC)_{ar}$
not present	not visible	1477w	1487	1487	1486	$\nu(CC)_{ar}$ or ν(C–O)(semiquinone)[20]
N/A	1522 (~1560 –1522)	1520	1524	1523	1524	$\nu_{as}(COO^-)$
1416, 1373	1434, 1370	1444, 1358	not resolvable	1420sh	1423sh	β(C–OH) (O=C–OH) or (Ar–OH)
N/A	1399 (~1399 –1370)	1407	1406	1400	1400	$\nu_{s}(COO^-)$
1308, 1277	1301w, 1281	1285, 1262	1262	1262	1262	ν(C–O) (O=C–OH) + $\nu(CC)_{ar}$ (14)[a, 14] or ν(C–H) (7a)[14]
1244	1254	1238, 1212	1216	1216	1217	ν(C–O) (Ar–OH)[15]
1188	1201	1190	1216	1216	1217	ν(C–H) (13)[14]

1167, 1114	1155, 1118, 1020	1173, 1148, 1111	1148, 1118, 1038	1147, 1118, 1017	1147, 1118	$\beta(C–H)_{ar}$
952, 924, or 901	941, 931	936, 925	933w	934w	not visible	γ(C–OH) (O=C–OH dimer, wag)[3, 15] or ν(C–H) (7b)[14]
901, 870	866	896, 877	883	888	889	γ(C–H) (5)[14] or lone H wag (1,3,4 substitution)[3, 4]
805[4]	802	797	796	796	796	γ(C–H) (11)[14] or 2 adjacent H wag (1,3,4 substitution)[3]
725 or 711	737, 716	~717sh	not visible	not visible	not visible	α(CCC) (1)[14] (radial skeletal) or ring pucker[3]
N/A	N/A	~600–567	586	579	580	ν(Fe–O)

[a]Numbers in brackets correspond to vibrational modes outlined in Láng and Varsányi.[14]

Key:
br, broad; w, weak; sh, shoulder.
ν, stretch; β, in-plane bend; γ, out-of-plane bend.
as, asymmetric; s, symmetric.
not visible: A given band was not visible but may be part of a larger broad absorption in the area. The band may exist but this cannot be confirmed or denied.
N/A: not applicable.

Table S9. Observed Bands (cm^{-1}) and Tentative Assignments from 4000–400 cm^{-1} for 2,3-Dihydroxybenzoic Acid (2,3-DHBA), the Sodium Salt of 2,3-DHBA (Na-2,3-DHB), and IONP-2,3-DHBA

2,3-DHBA	Na-2,3-DHB	IONP-2,3-DHBA		Tentative assignments
		HCl	DI water	
~3500–2400br	~3100–2400br	3368br	3351br	ν(O–H)
N/A	N/A	2927	2923	$\nu_{as}(CH_2)$
N/A	N/A	2856	2853	$\nu_{s}(CH_2)$
1678, 1656	1644w	not visible[a]	not visible[a]	ν(C=O)[23] (dimer)
1599, 1471[25, 26]	1606, 1477	1584, 1476	1584, 1476	$\nu(CC)_{ar}$ [23, 24]
N/A	1568	1543	1537	$\nu_{as}(COO^-)$[24a]
1433, 1381,[23] 1349[23, 24]	1383, 1355	not visible	not visible	β(C–OH) (O=C–OH or Ar–OH)
N/A	1421	1391	1397	$\nu_{s}(COO^-)$
1298	1298	not present	not present	ν(C–O) (O=C–OH)
1277	1276	not visible	not visible	β(C–H) (3)[b, 14] (rotation) or $\nu(CC)_{ar}$ (14)[14]
1255,[23] 1232	1230	1258, 1233	1257, 1231	ν(C–O) (Ar–OH)[15, 27]
1172sh, 1158, 1072	1196, 1160, 1088	1157, 1068	1157, 1068	β(C–H)[16, 23]
945	not present	not present	not visible	γ(C–OH) (O=C–OH dimer, wag)[3, 15]
792, 740, 722	792, 759, 724	794, 783, 755	794, 780, 754	γ(C–H) (wag, 3 adjacent H, 1,2,3 substitution)[3, 4]
792	792	783	794, 780	α(CCC) (12)[14] (radial skeletal)
792 or 740	792, 759	794, 755	794, 754	γ(C–H) (11)[14]
740 or 722	724	755	754	γ(CCC) (4)[14]
N/A	N/A	579	579	ν(Fe–O)

[a]Absorbance is wide in this area.

[b]Numbers in brackets correspond to vibrational modes outlined in Láng and Varsányi.[14]

Key:
br: broad.
ν, stretch; β, in-plane bend; γ, out-of-plane bend; α, aromatic in-plane deformation.
as, asymmetric; s = symmetric.
not visible: A given band was not visible but may be part of a larger broad absorption in the area. The band may exist but this cannot be confirmed or denied.
not present: A given band was not visible and is unlikely to be part of a larger broad overlapping absorption.
N/A: not applicable.

Table S10. Observed Bands (cm^{-1}) and Tentative Assignments from 4000–400 cm^{-1} for 2,5-Dihydroxybenzoic Acid (2,5-DHBA) and IONP-2,5-DHBA

2,5-DHBA	IONP-2,5-DHBA		Tentative assignments
	HCl	DI water	
3119br	3339br	3233br	ν(O–H)[28]
N/A	not visible	2927	$\nu_{as}(CH_2)$
N/A	not present	2858	$\nu_{s}(CH_2)$
1664[23, 28, 29]	not visible	not visible	ν(C=O)[14] (dimer)
1623	1628sh	1630sh	$\nu(CC)_{ar}$[23, 30] (8b)[a, 14]
1610[29a] or 1594[14]	not visible	not visible	$\nu(CC)_{ar}$[23] (8a)[24a]
N/A	1628sh,[b] 1548[29a]	1630sh, 1541[29a]	$\nu_{as}(COO^-)$
1496	1483	1481	$\nu(CC)_{ar}$[30] (19b)[14, 29a]
1469	not visible	not visible	$\nu(CC)_{ar}$[23]
1439	not visible	not visible	$\nu(CC)_{ar}$[23] (19a)[14]
N/A	1459, 1387	1454, 1386	$\nu_{s}(COO^-)$[29a]
1380	not visible	not visible	β(C–OH)[14]
not visible	~1351sh	~1350sh	$\nu(CC)_{ar}$ (14) or $\nu_{s}(COO^-)$
1277	1271	1273sh	ν(C–O)[14] (O=C–OH) + β(C–H) (3)[29a] (rotation)
1237	1236	1223	ν(C–O) (Ar–OH)[29a] (2-OH and 5-OH) + ν(C–H) (7a)[14]
1186br	not visible	not visible	ν(C–O) (Ar–OH)[16] or ν(C–H) (13)[14]
1137sh	1136	1135	β(C–H)[24a, 30] (18a[14] or 9b[29a])
1076	1086	1086	β(C–H) (18b[14] or 15[29a])
950	946	946	γ(C–H)[29a] (17b)[14]
932	not present	not present	ν(C–H) (7b)[14] or γ(C–OH) (O=C–OH dimer, wag)[3, 15]
not visible	885	886	γ(C–H)[29a] (5)[14] or lone H wag (1,2,5 substitution)[3, 4] or $\beta_{s}(COO^-)$[29b]

853	not present	not present	γ(C–OH)[14, 29b] (COOH)
833	825	826	γ(C–H)[4, 29a] (11)[14]
796	783	784	α(CCC) (12) (radial skeletal)[14]
787	783	784	γ(C–H) (2 adjacent H wag, 1,2,5 substitution)[3] or γ(C=O)[30]
755	not present	not present	β(C=O)[14, 29b] or ring deformation[30]
721	not visible	not visible	α(CCC) (1),[14] or γ(C–H)[30]
678	not visible	not visible	γ(C=O)[14, 30]
N/A	580	579	*ν*(Fe–O)
549	not visible	not visible	α(CCC) (6a)[14]
469	not visible	not visible	α(CCC) (6b)[14]
407	not visible	not visible	β(C–H) (9b)[14]

[a]Numbers in brackets correspond to vibrational modes outlined in Láng and Varsányi.[14]
[b]Underlined values for bands are the more likely choice for the assignment.

Key:
br, broad; sh, shoulder.
ν, stretch; β, in-plane bend; γ, out-of-plane bend; α, aromatic in-plane deformation.
as, asymmetric; s, symmetric.
not visible: A given band was not visible but may be part of a larger broad absorption in the area. The band may exist but this cannot be confirmed or denied.
not present: A given band was not visible and is unlikely to be part of a larger broad overlapping absorption.
N/A: not applicable.

Table S11. Observed Bands (cm^{-1}) and Tentative Assignments from 4000–400 cm^{-1} for Salicylic Acid (SA), and IONP-SA

Salicylic acid (SA)	IONP-SA (HCl)	IONP-SA (DI water)	Tentative assignments
~3300–2400br	3252br	3202br	ν(O–H)
3062sh	not visible	not visible	ν(C–H)[31] (20a)[a, 14]
N/A	2925w	2925	$\nu_{as}(CH_2)$
N/A	2857w	2854	$\nu_{s}(CH_2)$
1655[32]	not visible	not visible	ν(C=O)[14, 23, 33] (dimer)
1610[23, 32]	1620 or 1602[31, 34]	1621 or 1601[31, 34]	$\nu(CC)_{ar}$[34] (8b)[14, 35]
1579[23, 32]	1584sh	1582w	$\nu(CC)_{ar}$[31] (8a)[14, 33, 35]
not visible	1602, 1527	1601, 1527	$\nu_{as}(COO^-)$
1482[23, 32, 36]	1482sh, w	1481sh, w	$\nu(CC)_{ar}$[37] (19b)[14, 28, 35]
1465[23, 32]	1468	1468	$\nu(CC)_{ar}$[31, 34] (19a)[14, 33]
1443	1455	1456	$\nu(CC)_{ar}$[15, 23] or β(C–OH)[14] (O=C–OH)[32]
N/A	~1409sh, w; 1390	~1409sh, w; 1390	$\nu_{s}(COO^-)$
1383w	not visible	not visible	β(C–OH) (Ar–OH)[32]
1324[14]	~1354sh	~1349sh	$\nu(CC)_{ar}$ (14)
1324	not visible	not visible	$\nu(CC)_{ar}$ (14)[14] or ν(C–O) (O=C–OH)[32, 33]
1292	not visible	not visible	ν(C–O) (O=C–OH)[14] + β(C–H) (3)[33] (rotation)
1247	1246	1248	ν(C–O) (Ar–OH)[23, 32–36, 37] or ν(C–H) (7a)[14]
1209	not present	not visible	β(C–OH)[14, 23] or ν(C–O) (Ar–OH)[16]
1188	not present	~1188sh	ν(C–H) (13)[14]
1155	1159	1159	β(C–H)[23, 35, 37] (9a)[14, 33]

not visible	1144	1144	β(C–H)[35, 37a] (18a)[14, 37b] (9b)[33]
1089	not visible	1095	β(C–H)[23] (15)[33]
1030	1033	1032	β(C–H)[15, 23, 35, 37a] (18b[14, 32, 37b] or 18a[33]) (translation)
994	not visible	not visible	γ(C–H) (5)[14]
964	not visible	not visible	γ(C–H) (17b)[14]
867	864sh	865sh	$\beta_s(COO^-)$[38] or γ(C–H) (10a)[33]
852	not present	not present	α(CCC) (12) (radial skeletal)[14]
784	794	793	α(CCC) (1) (radial skeletal)[14]
757	756	755	γ(C–H)[31] (11)[14] or 4 adjacent CH wag (ortho substitution)[3, 4, 15]
693	~701sh, w	701sh	ϕ(CCC) (4) (skeletal)[14]
659	~660sh, w	~661sh, w	γ(C=O)[14]
N/A	579	579	*ν*(Fe–O)
567	not visible	not visible	α(CCC) (6a)[33] (radial skeletal)[14]
531	not visible	not visible	ϕ(CCC) (16a) (skeletal)[14]
463	not visible	not visible	α(CCC) (6b) (radial skeletal)[14]
430	not visible	not visible	ϕ(CCC) (16b) (skeletal)[14]

[a]Numbers in brackets correspond to vibrational modes outlined in Láng and Varsányi.[14]

Key:

br, broad; w, weak; sh, shoulder.

ν, stretch; β, in-plane bend; γ, out-of-plane bend; α, aromatic in-plane deformation; ϕ, aromatic out-of-plane deformation.

as, asymmetric; s, symmetric.

ar: aromatic ring.

not visible: A given band was not visible but may be part of a larger broad absorption in the area. The band may exist but this cannot be confirmed or denied.

not present: A given band was not visible and is unlikely to be part of a larger broad overlapping absorption.

Table S12. Observed Bands (cm^{-1}) and Tentative Assignments from 4000–400 cm^{-1} for 2,4-Dihydroxybenzoic Acid (2,4-DHBA), the Sodium Salt of 2,4-DHBA (Na-2,4-DHB), and IONP-2,4-DHBA

2,4-DHBA	Na-2,4-DHB	IONP-2,4-DHBA			Tentative assignments
		(HCl)	(HCl) (6 washes acetone)	(DI water)	
~3300–2550br	~3575–2570br	3194br	3213br	3152br	ν(O–H)[28]
N/A	N/A	2926	not resolvable	2924	$\nu_{as}(CH_2)$
N/A	N/A	not resolvable	not resolvable	2855	$\nu_{s}(CH_2)$
not present	not present	1719	not present	not present	ν(C=O)
1629br	1636	1627	1627	1625	ν(C=O) (dimer) + $\nu(CC)_{ar}$[39] (8b)[a, 14]
N/A	1557	1599	1602	1600	$\nu_{as}(COO^-)$
1521	1515	1534w or 1509	1530w or 1509	1520w or 1508	$\nu(CC)_{ar}$[39] (19b)[14]
1444	1441	1456	1457	1455	$\nu(CC)_{ar}$[39] (19a)[14]
1406	1408	not visible	not visible	not visible	β(C–OH)[14, 39]
N/A	1483 or 1345[b]	1387	1389	1386	$\nu_{s}(COO^-)$
1352	1345	not visible	not visible	not visible	$\nu(CC)_{ar}$ (14)[14]
1280	1300	1294	1298, 1276vw[c]	1295	ν(C–O) (O=C–OH) + β(C–H) (3) (rotation)[14]
not visible	1263	1248	1251, 1276vw	1249	ν(C–O) (Ar–OH)[16] (2-OH)
1225	1222	not resolvable	not resolvable	not resolvable	ν(C–O) (Ar–OH)[16] (4-OH)
1185	1185	not visible	1177	1177	ν(C–H) (13)[14]
1157	1147	1155	1158	1157	β(C–H)[39] (18a)

					(translation)[14]
1092	1091	1102	1104	1102	β(C–H) (18b) (translation)[14]
978	984	988 or 976	988 or 977	988 or 976	*ν*(C–H) (7b)[14]
951	not present	949	not visible	not visible	γ(C–H) (17b)[14]
875	860	883	883	884	γ(C–H) (5)[14] (lone H wag, 1,2,4 substitution)[3,4] or γ(OH)[14]
846	860 or 828	849	849	847	γ(C–H)[4, 39] (11)[14]
772	761	783	782	780	α(CCC) (12) (radial skeletal)[14] or 2 adjacent H wag (1,2,4 substitution)[3]
748	761	not visible	not visible	not visible	β(C=O)[14]
687	688	~694sh	~694sh	~693sh	ϕ(CCC) (4) (skeletal),[14] ring pucker[3]
N/A	N/A	571	572	567	*ν*(Fe–O)
478	482	not visible	not visible	not visible	ϕ(CCC) (16b) (skeletal)[14]

[a]Numbers in brackets correspond to vibrational modes outlined in Láng and Varsányi.[14]
[b]Underlined value is the more likely choice for the assignment.
[c]Vibration may correspond to deprotonated phenol.[40]

Key:
br, broad; vw, very weak.
ν, stretch; β, in-plane bend; γ, out-of-plane bend; α, aromatic in-plane deformation; ϕ, aromatic out-of-plane deformation.
as, asymmetric; s, symmetric.
ar: aromatic ring.
not resolvable: A given band is extremely weak or appears to be contained within a wider absorbance and its exact position cannot be resolved.
not visible: A given band was not visible but may be part of a larger broad absorption in the area. The band may exist but this cannot be confirmed or denied.
not present: A given band was not visible and is unlikely to be part of a larger broad overlapping absorption.
N/A: not applicable.

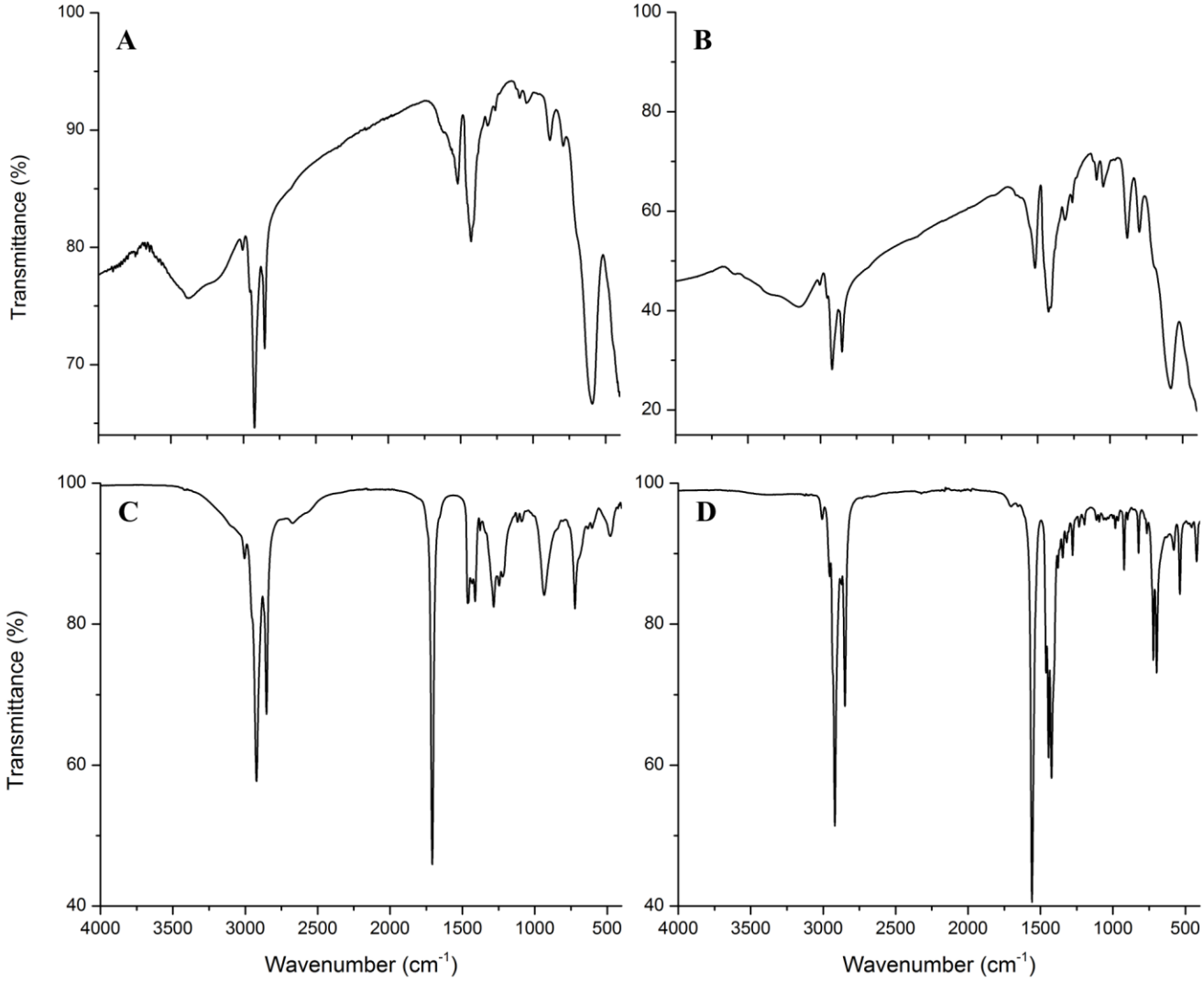

Figure S4. FTIR spectra of (A) IONP-OA (Batch 1), with select bands as follows (in cm^{-1}): 3378br ν(OH); 3006 ν(=CH)$_{vinyl}$; 2954 $\nu_{as}(CH_3)$; 2923 $\nu_{as}(CH_2)$; 2858 $\nu_s(CH_2)$; 1520 $\nu_{as}(COO^-)$; 1428 $\nu_s(COO^-)$; ~1379sh $\delta_s(CH_3)$; 1262w $\nu(CO)_{O=C-OH}$; 591 ν(Fe–O).
(B) IONP-OA (Batch 2): 3152br ν(OH); 3004 ν(=CH)$_{vinyl}$; 2954 $\nu_{as}(CH_3)$; 2920 $\nu_{as}(CH_2)$; 2851 $\nu_s(CH_2)$; 1519 $\nu_{as}(COO^-)$; 1425 $\nu_s(COO^-)$; ~1379sh $\delta_s(CH_3)$; 1261w $\nu(CO)_{O=C-OH}$; 580 ν(Fe–O).
(C) oleic acid (liquid, neat): ~3330–2400br ν(OH); 3005 ν(=CH)$_{vinyl}$; ~2955sh $\nu_{as}(CH_3)$; 2922 $\nu_{as}(CH_2)$; 2853 $\nu_s(CH_2)$; 1708 ν(C=O); 1464 $\beta_s(CH_2)_{scissor}$ or β(COH); 1377 $\delta_s(CH_3)$; 1284 $\nu(CO)_{O=C-OH}$.
(D) sodium oleate solid: 3007 ν(=CH)$_{vinyl}$; 2956 $\nu_{as}(CH_3)$; 2919 $\nu_{as}(CH_2)$; 2874 $\nu_s(CH_3)$; 2850 $\nu_s(CH_2)$; 1559 $\nu_{as}(COO^-)$; 1444 or 1424 $\nu_s(COO^-)$; 1379 $\delta_s(CH_3)$; 1278w $\nu(CO)_{O=C-OH}$.

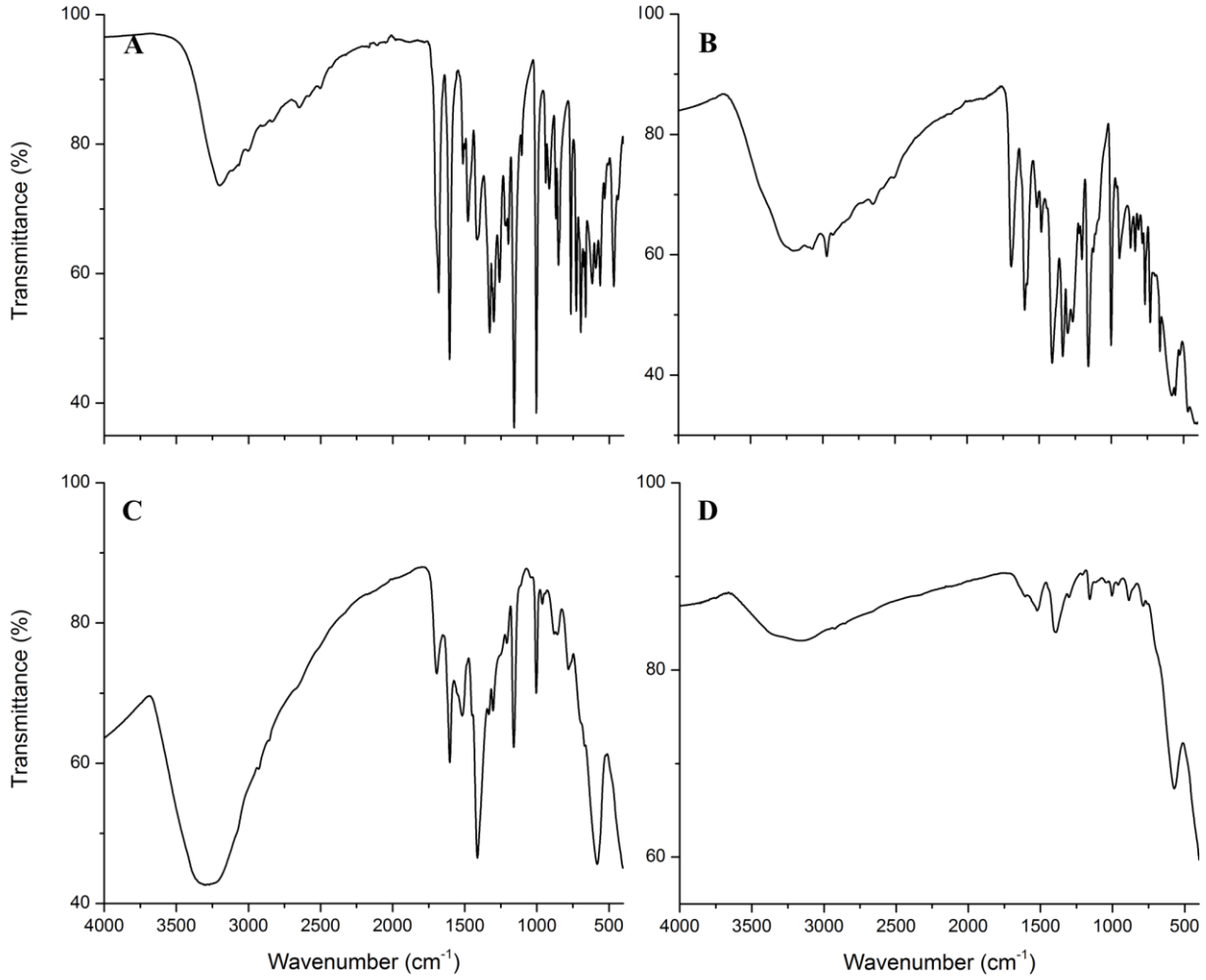

Figure S5. FTIR spectra of (A) 3,5-DHBA solid, with select bands as follows (in cm^{-1}): 3199br ν(OH); 1682 ν(C=O), $\nu(CC)_{ar}$; 1606, 1514 $\nu(CC)_{ar}$; 1479 $\nu(CC)_{ar}$, β(COH); 1415 β(COH); 1415 $\beta(COH)_{Ar–OH}$; 1300 ν(CH); 1260 $\nu(CO)_{O=C–OH}$, $\nu(CC)_{ar}$; 1199 $\nu(CO)_{Ar–OH}$; 1159 β(CH); 1005 α(CCC).
(B) IONP-3,5-DHBA (HCl preparation): 3202br ν(OH); 2930w $\nu_{as}(CH_2)$; 1693 ν(C=O), $\nu(CC)_{ar}$; 1600, 1517 $\nu(CC)_{ar}$; 1584sh $\nu_{as}(COO^-)$; 1485 $\nu(CC)_{ar}$, β(COH); 1410 β(COH); 1337 $\beta(COH)_{Ar–OH}$; 1303 ν(CH); 1267 $\nu(CO)_{O=C–OH}$, $\nu(CC)_{ar}$; 1204 $\nu(CO)_{Ar–OH}$; 1159 β(CH); 1002 α(CCC); 580 ν(Fe–O).
(C) IONP-3,5-DHBA (DI water): 3306br ν(OH); 2929w $\nu_{as}(CH_2)$; 2858w $\nu_s(CH_2)$; 1694 ν(C=O), $\nu(CC)_{ar}$; 1603, 1518 $\nu(CC)_{ar}$, ~1552sh $\nu_{as}(COO^-)$; 1412 β(COH); 1333 $\beta(COH)_{Ar–OH}$, 1304 ν(CH); 1208 $\nu(CO)_{Ar–OH}$; 1160 β(CH); 1004 α(CCC); 582 ν(Fe–O).
(D) IONP-3,5-DHBA (DI water, with DI water wash): 3159br ν(OH); 1605, 1523 $\nu(CC)_{ar}$, 1523 $\nu_{as}(COO^-)$; 1396 $\nu_s(COO^-)$; 1302 ν(CH); 1209 $\nu(CO)_{Ar–OH}$; 1158 β(CH); 1005 α(CCC); 572 ν(Fe–O).

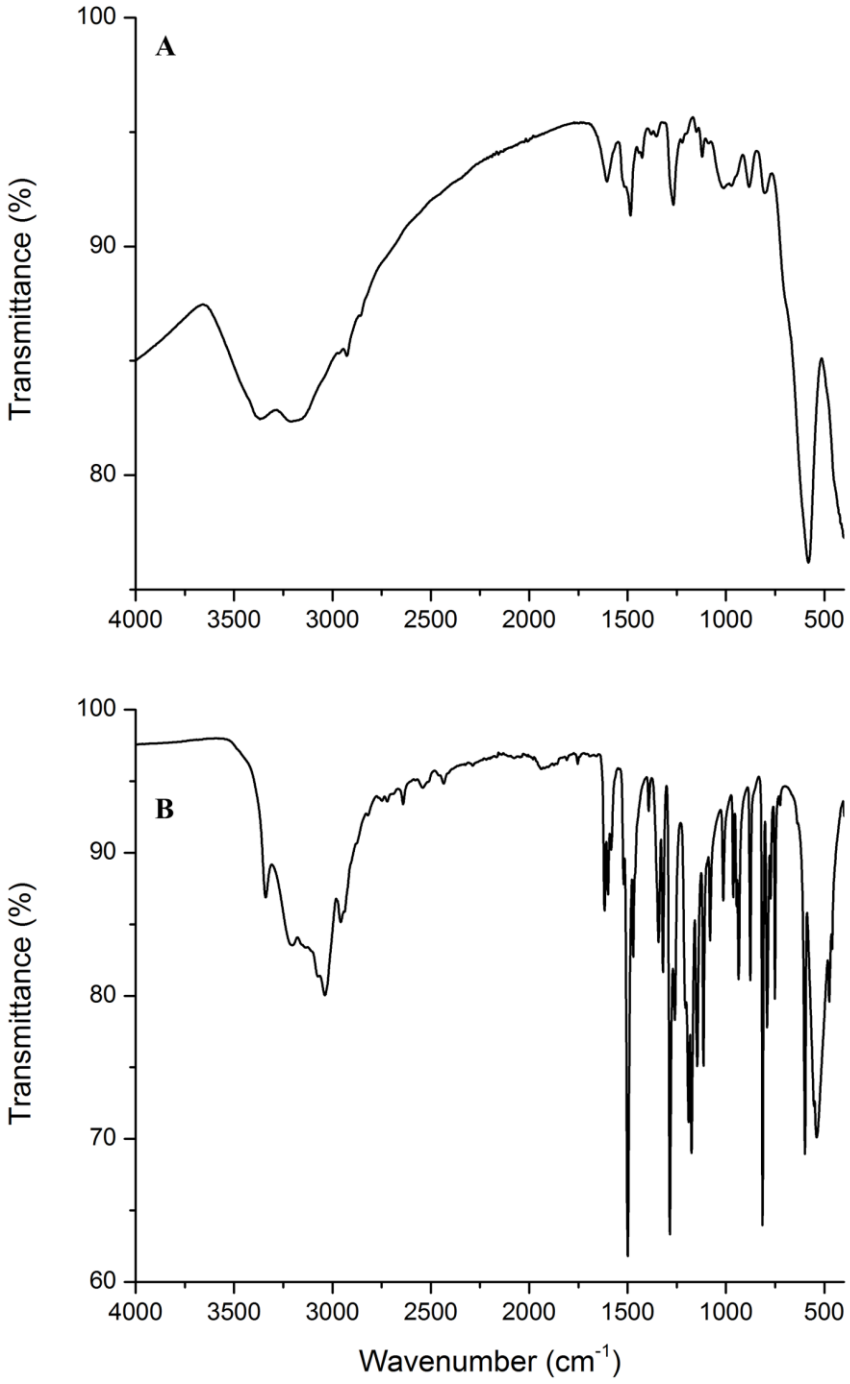

Figure S6. FTIR spectra of (A) IONP-DA, with select bands as follows (in cm^{-1}): 3213br ν(OH), $\nu(NH_2)$; 2927 $\nu_{as}(CH_2)$; 2858 $\nu_s(CH_2)$; 1605 $\delta_s(NH_2)_{scissor}$; 1485 $\nu(CC)_{ar}$; 1485 $\nu(CO)_{semiquinone}$; 1427w $\nu(COO^-)_{as}$, 1267 $\gamma_{as}(CH_2)_{twist}$ or β(CCN); 1222w β(CCN); ~1202sh, w ν(CC)+$\nu(CO)_{Ar–OH}$; 1150, 1121 $\beta(CH)_{ar}$; 1088w ν(CCN), 1012 ν(CN), 803 $\gamma(NH)_{wag}$ or $\gamma(C–H)_{ar}$; 582 ν(Fe–O). (B) DA·HCl solid: 3339br ν(OH), $\nu(NH_2)$; 2929 $\nu_{as}(CH_2)$; 1600 $\delta_s(NH_2)_{scissor}$; 1617, 1584, 1499 $\nu(CC)_{ar}$; 1471 $\beta_s(CH_2)_{scissor}$ or $\nu(CC)_{ar}$; 1393, 1321 $\beta(COH)_{Ar–OH}$; 1261 $\gamma_{as}(CH_2)_{twist}$ or β(CCN); 1206w β(CCN); 1190, 1175 ν(CC)+$\nu(CO)_{Ar–OH}$; 1146, 1114 $\beta(CH)_{ar}$; 1081 ν(CCN), 1014 ν(CN) 791 $\gamma(NH)_{wag}$ or $\gamma(C–H)_{ar}$.

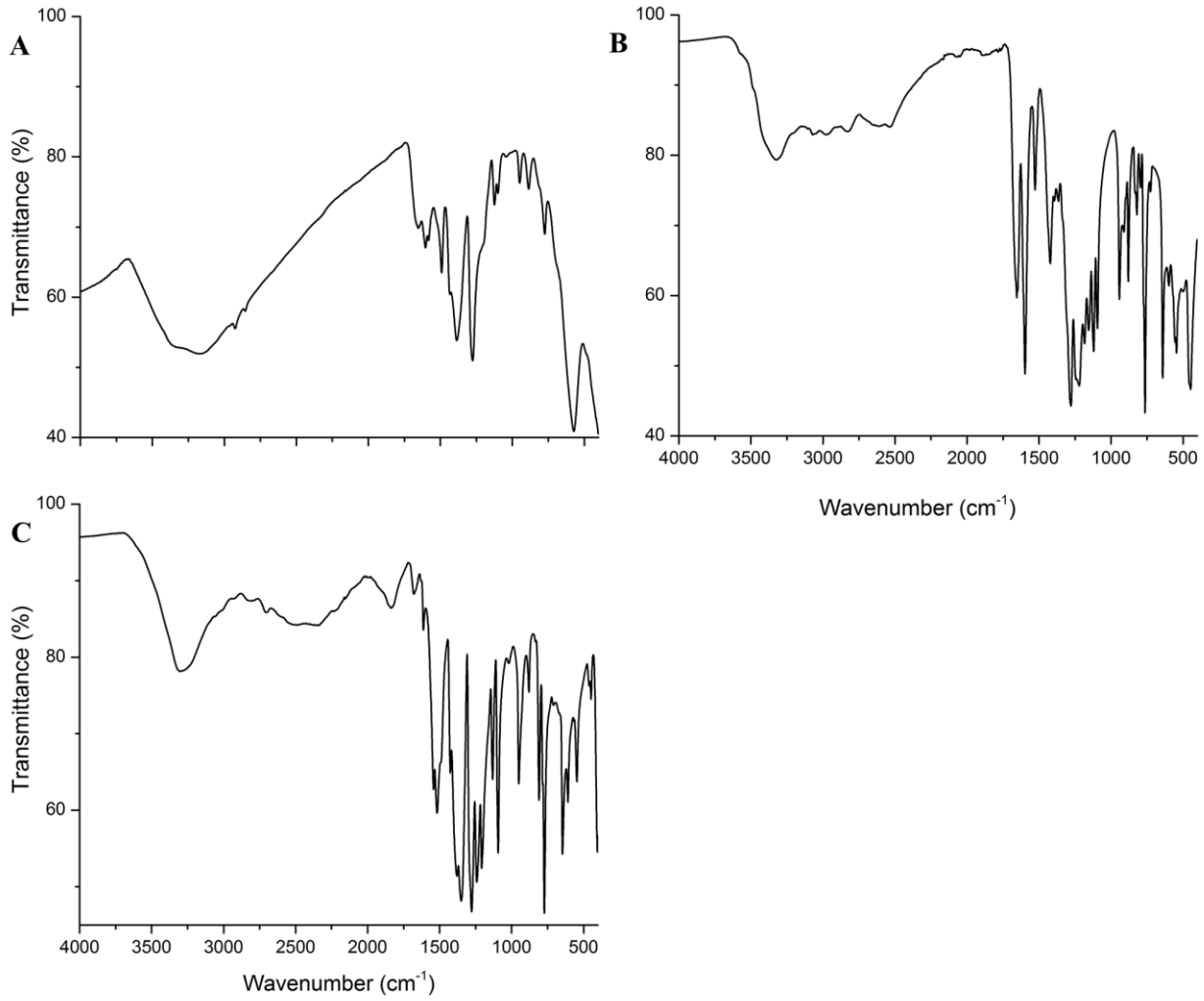

Figure S7. FTIR spectra of (A) IONP-3,4-DHBA (DI water), with select bands as follows (in cm^{-1}): 3168br ν(OH); 2825 $\nu_{as}(CH_2)$; 2855 $\nu_s(CH_2)$; 1654 $\nu(C{=}O)_{dimer}$; 1603, 1432sh $\nu(CC)_{ar}$; 1582 $\nu_{as}(COO^-)$; 1491 $\nu(CC)_{ar}$ or $\nu(CO)_{semiquinone}$; 1388 $\beta(COH)_{O=C-OH\ or\ Ar-OH}$; 1388 $\nu_s(COO^-)$; 1276 $\nu(CO)_{O=C-OH}$ + ν(CH); 1124 ν(CH) or β(CH); 1100 β(CH); 949 ν(CH) or $\gamma(COH)_{O=C-OH\ dimer,\ wag}$; 572 ν(Fe–O).
(B) 3,4-DHBA (solid): 3320br, 2534 ν(OH); 1654 $\nu(C{=}O)_{dimer}$; 1597, 1527, 1421 $\nu(CC)_{ar}$; 1392, 1364 $\beta(COH)_{O=C-OH\ or\ Ar-OH}$; ~1307sh, 1278 $\nu(CO)_{O=C-OH}$ + ν(CH); 1244sh, 1221 $\nu(CO)_{Ar-OH}$; 1155, 1094 β(CH); 1120 ν(CH) or β(CH); 942 ν(CH); 942 or 910 $\gamma(COH)_{O=C-OH\ dimer,\ wag}$.
(C) Na-3,4-DHB: 3305br ν(OH); 1679w $\nu(C{=}O)_{dimer}$; 1613, 1518, 1426 $\nu(CC)_{ar}$; 1541 $\nu_{as}(COO^-)$; ~1490sh $\nu(CC)_{ar}$ or $\nu(CO)_{semiquinone}$; 1380 $\nu_s(COO^-)$; 1350 $\beta(COH)_{O=C-OH\ or\ Ar-OH}$; 1278 $\nu(CO)_{O=C-OH}$ + ν(CH); 1242, 1208 $\nu(CO)_{Ar-OH}$; 1132 ν(CH) or β(CH); 1094 β(CH); 950 ν(CH) or $\gamma(COH)_{O=C-OH\ dimer,\ wag}$.

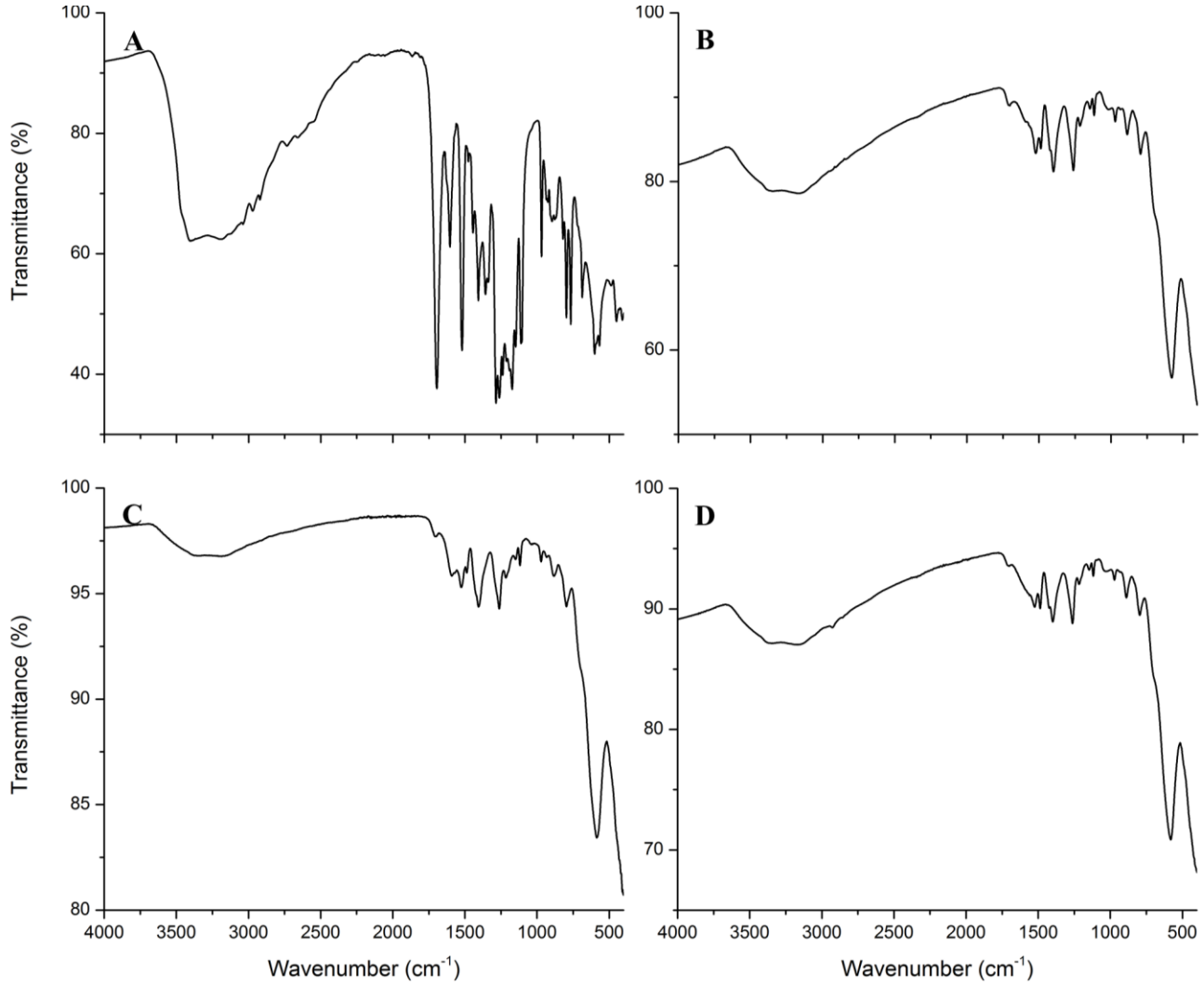

Figure S8. FTIR spectra of (A) IONP-3,4-DHPA (HCl preparation), with select bands as follows (in cm^{-1}): 3405br ν(OH); 1694 ν(C=O); 1604, 1520 $\nu(CC)_{ar}$; 1477w $\nu(CC)_{ar}$ or $\nu(CO)_{semiquinone}$; 1520 $\nu_{as}(COO^-)$; 1444, 1358 $\beta(COH)_{O=C-OH\ or\ Ar-OH}$; 1407 $\nu_s(COO^-)$; 1285, 1262 $\nu(CO)_{O=C-OH}$ + $\nu(CC)_{ar}$ or ν(CH); 1238, 1212 $\nu(CO)_{Ar-OH}$; 1173, 1148, 1111 $\beta(CH)_{ar}$; 936, 925 $\gamma(COH)_{O=C-OH\ dimer,\ wag}$ or ν(CH); ~600–567 ν(Fe–O).
(B) IONP-3,4-DHPA (DI water): 3165br ν(OH); 1702 ν(C=O); 1590, 1523 $\nu(CC)_{ar}$; 1487 $\nu(CC)_{ar}$ or $\nu(CO)_{semiquinone}$; 1523 $\nu_{as}(COO^-)$; 1420sh $\beta(COH)_{O=C-OH\ or\ Ar-OH}$; 1400 $\nu_s(COO^-)$; 1262 $\nu(CO)_{O=C-OH}$ + $\nu(CC)_{ar}$ or ν(CH); 1216 $\nu(CO)_{Ar-OH}$ or ν(CH); 1147, 1118, 1017 $\beta(CH)_{ar}$; 934w $\gamma(COH)_{O=C-OH\ dimer,\ wag}$ or ν(CH); 579 ν(Fe–O).
(C) IONP-3,4-DHPA (HCl, 2x washed): 3188br ν(OH); 1700 ν(C=O); 1591, 1524 $\nu(CC)_{ar}$; 1487 $\nu(CC)_{ar}$ or $\nu(CO)_{semiquinone}$; 1524 $\nu_{as}(COO^-)$; 1406 $\nu_s(COO^-)$; 1262 $\nu(CO)_{O=C-OH}$ + $\nu(CC)_{ar}$ or ν(CH); 1216 $\nu(CO)_{Ar-OH}$ or ν(CH); 1148, 1118, 1038 $\beta(CH)_{ar}$; 933w $\gamma(COH)_{O=C-OH\ dimer,\ wag}$ or ν(CH); 586 ν(Fe–O).
(D) IONP-3,4-DHPA (DI water, 2x washed): 3180br ν(OH); 2926w $\nu_{as}(CH_2)$; 1702 ν(C=O); 1590, 1523 $\nu(CC)_{ar}$; 1486 $\nu(CC)_{ar}$ or $\nu(CO)_{semiquinone}$; 1524 $\nu_{as}(COO^-)$; 1423sh $\beta(COH)_{O=C-OH\ or\ Ar-OH}$; 1400 $\nu_s(COO^-)$; 1262 $\nu(CO)_{O=C-OH}$ + $\nu(CC)_{ar}$ or ν(CH); 1217 $\nu(CO)_{Ar-OH}$ or ν(CH); 1147, 1118 $\beta(CH)_{ar}$; 580 ν(Fe–O).

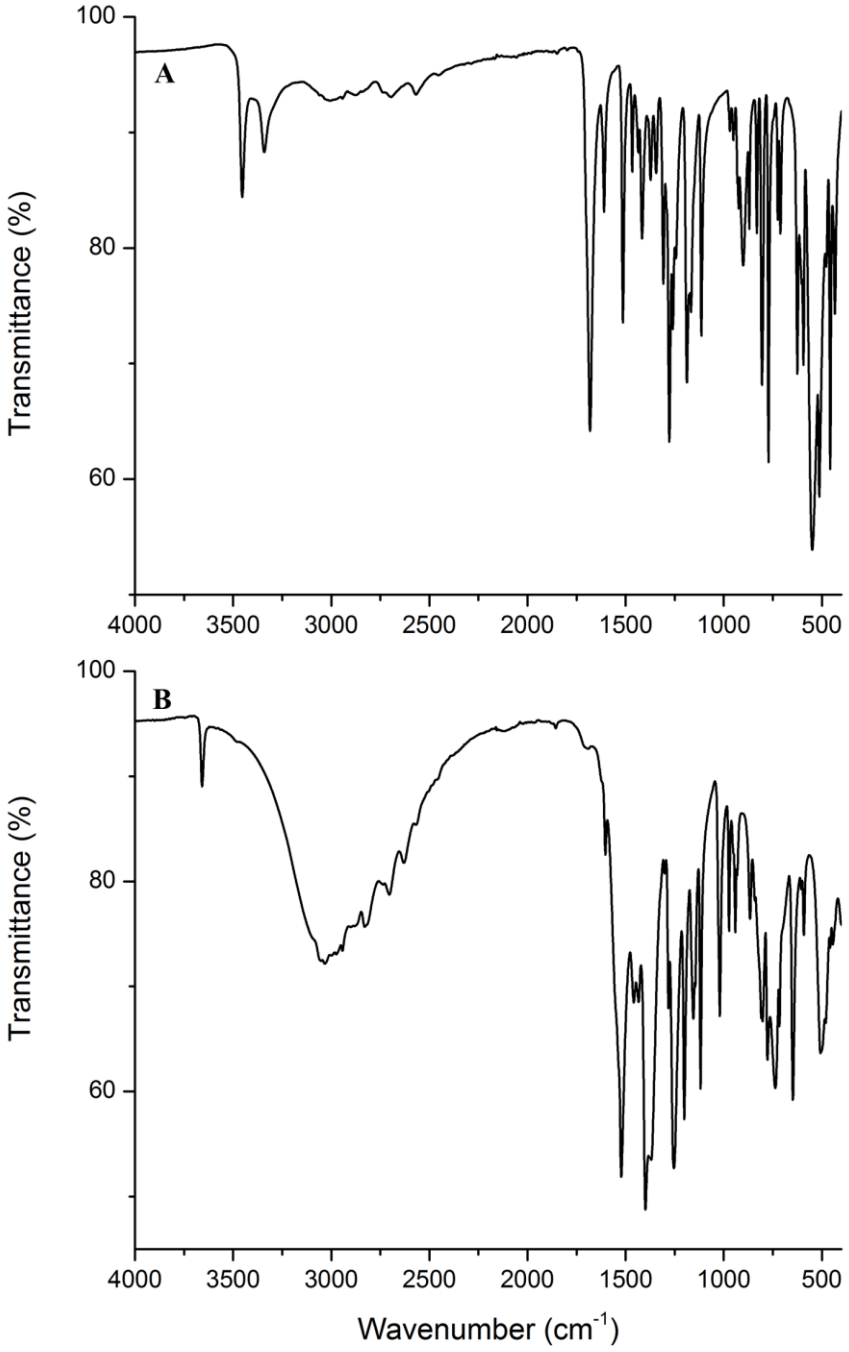

Figure S9. FTIR spectra of (A) 3,4-DHPA solid, with select bands as follows (in cm^{-1}): ~3475–2400br ν(OH); 2943 $\nu_{as}(CH_2)$; 2843w $\nu_s(CH_2)$; 1682 ν(C=O); 1610, 1514, 1466 $\nu(CC)_{ar}$; 1416, 1373 $\beta(COH)_{O=C-OH\ or\ Ar-OH}$; 1308, 1277 $\nu(CO)_{O=C-OH}$ + $\nu(CC)_{ar}$ or ν(CH); 1244 $\nu(CO)_{Ar-OH}$; 1188 ν(CH); 1167, 1114 $\beta(CH)_{ar}$; 952, 924, or 901 $\gamma(COH)_{O=C-OH\ dimer,\ wag}$ or ν(CH).
(B) sodium salt of 3,4-DHPA (Na-3,4-DHP): 3658, 3032br ν(OH); 2943 $\nu_{as}(CH_2)$; 2830 $\nu_s(CH_2)$; 1603, 1522, 1458 $\nu(CC)_{ar}$; 1522 (~1560–1522) $\nu_{as}(COO^-)$; 1434, 1370 $\beta(COH)_{O=C-OH\ or\ Ar-OH}$; 1399 (~1399–1370) $\nu_s(COO^-)$; 1301w, 1281 $\nu(CO)_{O=C-OH}$ + $\nu(CC)_{ar}$ or ν(CH); 1254 $\nu(CO)_{Ar-OH}$; 1155 ν(CH); 1155, 1118, 1020 $\beta(CH)_{ar}$; 941, 931 $\gamma(COH)_{O=C-OH\ dimer,\ wag}$ or ν(CH).

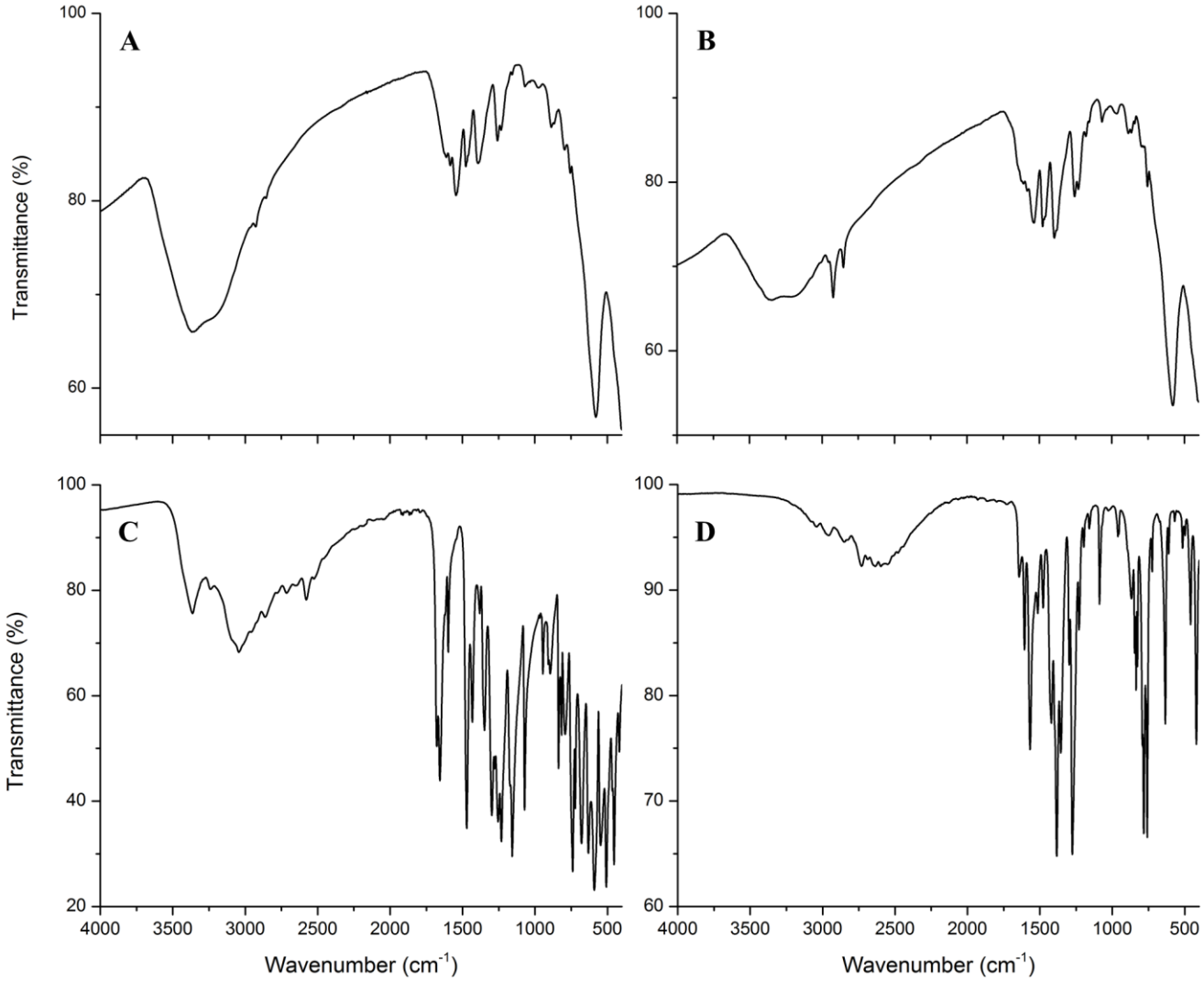

Figure S10. FTIR spectra of (A) IONP-2,3-DHBA (HCl preparation), with select bands as follows (in cm^{-1}): 3368br ν(OH); 2927 $\nu_{as}(CH_2)$; 2856 $\nu_s(CH_2)$; 1584, 1476 $\nu(CC)_{ar}$; 1543 $\nu_{as}(COO^-)$; 1391 $\nu_s(COO^-)$; 1258, 1233 $\nu(CO)_{Ar–OH}$; 1157, 1068 β(CH); 579 ν(Fe–O).
(B) IONP-2,3-DHBA (DI water): 3351br ν(OH); 2923 $\nu_{as}(CH_2)$; 2853 $\nu_s(CH_2)$; 1584, 1476 $\nu(CC)_{ar}$; 1537 $\nu_{as}(COO^-)$; 1397 $\nu_s(COO^-)$; 1257, 1231 $\nu(CO)_{Ar–OH}$; 1157, 1068 β(CH); 579 ν(Fe–O).
(C) 2,3-DHBA solid: ~3500–2400br ν(OH); 1678, 1656 $\nu(CO)_{dimer}$; 1599, 1471 $\nu(CC)_{ar}$; 1433, 1381, 1349 $\beta(COH)_{O=C–OH \text{ or } Ar–OH}$; 1298 $\nu(CO)_{O=C–OH}$; 1277 β(CH) or $\nu(CC)_{ar}$; 1255, 1232 $\nu(CO)_{Ar–OH}$; 1172sh, 1158, 1072 β(CH); 945 $\gamma(COH)_{O=C–OH}$.
(D) sodium salt of 2,3-DHBA (Na-2,3-DHB): ~3100–2400br ν(OH); 1644w $\nu(CO)_{dimer}$; 1606, 1477 $\nu(CC)_{ar}$; 1568 $\nu_{as}(COO^-)$; 1383, 1355 $\beta(COH)_{O=C–OH \text{ or } Ar–OH}$; 1421 $\nu_s(COO^-)$; 1298 $\nu(CO)_{O=C–OH}$; 1276 β(CH) or $\nu(CC)_{ar}$; 1230 $\nu(CO)_{Ar–OH}$; 1196, 1160, 1088 β(CH).

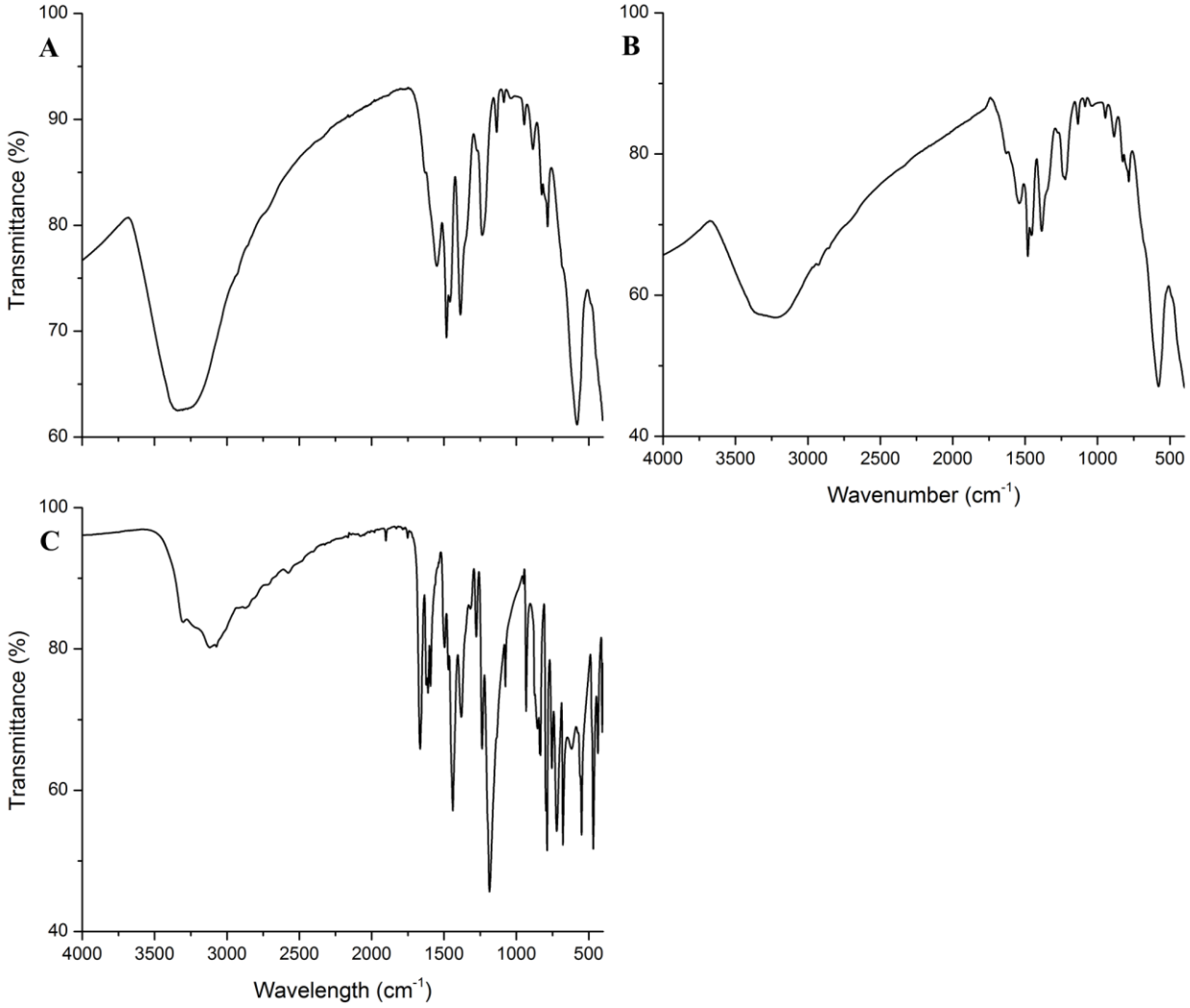

Figure S11. FTIR spectra of (A) IONP-2,5-DHBA (HCl preparation), with select bands as follows (in cm^{-1}): 3339br ν(OH); 1628sh, 1483 $\nu(CC)_{ar}$; 1628sh or 1548 $\nu_{as}(COO^-)$; 1459, 1387 $\nu_s(COO^-)$; ~1351sh $\nu(CC)_{ar}$ or $\nu_s(COO^-)$; 1271 $\nu(CO)_{O=C-OH}$ + β(CH); 1236 $\nu(CO)_{Ar-OH}$ + ν(CH); 1136, 1086 β(CH); 885 γ(CH) or $\beta_s(COO^-)$; 580 ν(Fe–O).
(B) IONP-2,5-DHBA (DI water): 3233br ν(OH); 2927 $\nu_{as}(CH_2)$; 2858 $\nu_s(CH_2)$; 1630sh, 1481 $\nu(CC)_{ar}$; 1630sh or 1541 $\nu_{as}(COO^-)$; 1454, 1386 $\nu_s(COO^-)$; ~1350sh $\nu(CC)_{ar}$ or $\nu_s(COO^-)$; 1273sh $\nu(CO)_{O=C-OH}$ + β(CH); 1223 $\nu(CO)_{Ar-OH}$ + ν(CH); 1135, 1086 β(CH); 886 γ(CH) or $\beta_s(COO^-)$; 579 ν(Fe–O).
(C) 2,5-DHBA solid: 3119br ν(OH); 1664 $\nu(CO)_{dimer}$; 1623, 1610, 1594, 1496, 1469, 1439 $\nu(CC)_{ar}$; 1380 β(COH); 1277 $\nu(CO)_{O=C-OH}$ + β(CH); 1237 $\nu(CO)_{Ar-OH}$ + ν(CH); 1186br $\nu(CO)_{Ar-OH}$ or ν(CH); 1076 β(CH); 932 ν(CH) or $\gamma(COH)_{O=C-OH\ dimer,\ wag}$; 853 $\gamma(COH)_{COOH}$; 755 β(C=O) or ring deformation; 678 γ(C=O).

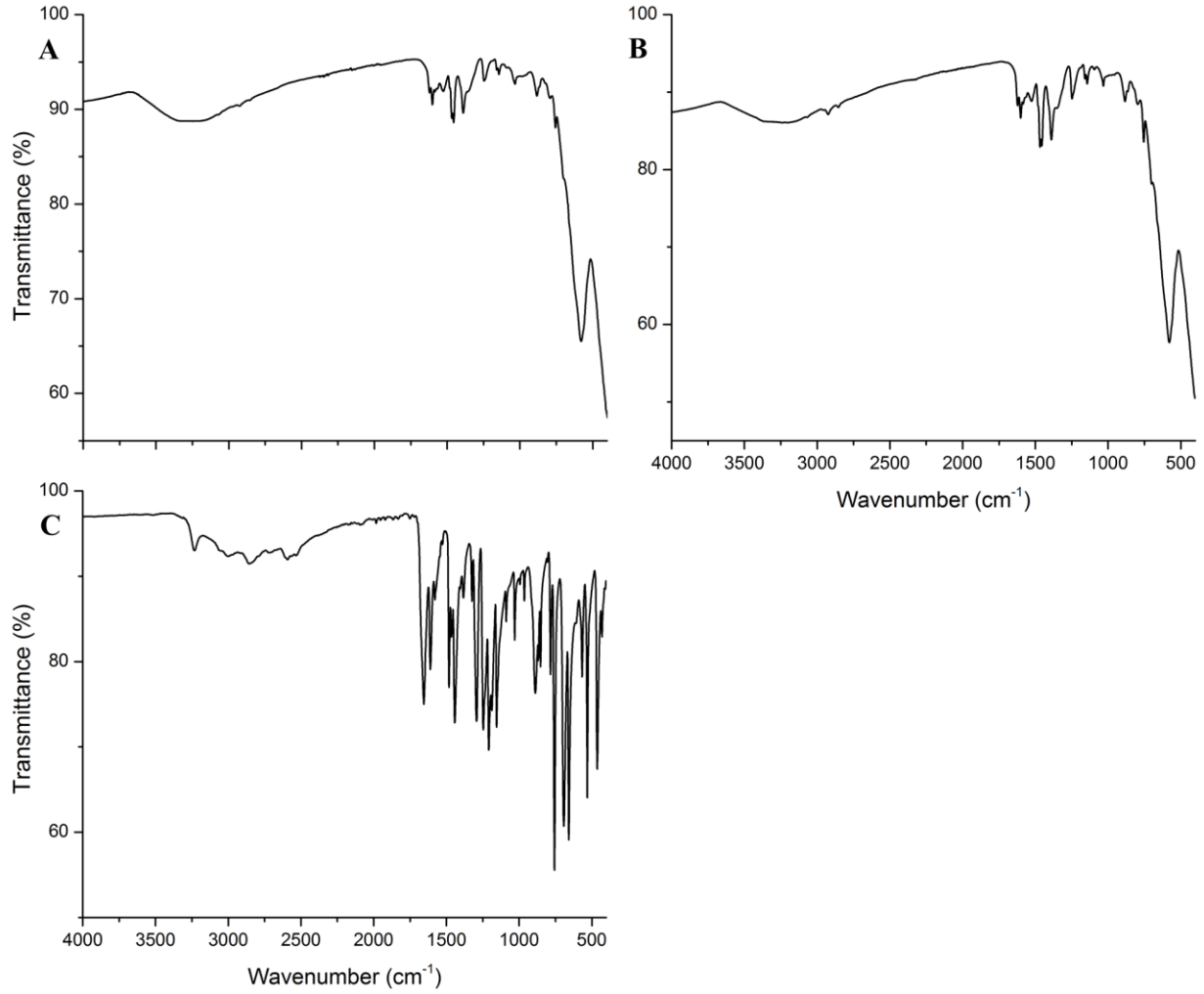

Figure S12. FTIR spectra of (A) IONP-SA (HCl preparation), with select bands as follows (in cm-1): 3253br ν(OH); 2825w $\nu_{as}(CH_2)$; 2857w $\nu_s(CH_2)$; 1620, 1584sh, 1482sh, w, 1468, ~1354sh $\nu(CC)_{ar}$; 1602 $\nu(CC)_{ar}$ or $\nu_{as}(COO^-)$; 1527 $\nu_{as}(COO^-)$; 1455 $\nu(CC)_{ar}$ or $\beta(COH)_{O=C-OH}$; ~1409sh, w, 1390 $\nu_s(COO^-)$; 1246 $\nu(CO)_{Ar-OH}$ or ν(CH); 1159, 1144, 1033 β(CH); 864sh $\beta_s(COO^-)$ or γ(CH); ~660sh, w γ(C=O); 579 ν(Fe–O).
(B) IONP-SA (DI water): 3202br ν(OH); 2925 $\nu_{as}(CH_2)$; 2854 $\nu_s(CH_2)$; 1621, 1582w, 1481sh, w, 1468, ~1349sh $\nu(CC)_{ar}$; 1601 $\nu(CC)_{ar}$ or $\nu_{as}(COO^-)$; 1527 $\nu_{as}(COO^-)$; 1456 $\nu(CC)_{ar}$ or $\beta(COH)_{O=C-OH}$; ~1409sh, w, 1390 $\nu_s(COO^-)$; 1248 $\nu(CO)_{Ar-OH}$ or ν(CH); ~1188sh ν(CH); 1159, 1144, 1095, 1032 β(CH); 865sh $\beta_s(COO^-)$ or γ(CH); ~661sh, w γ(C=O); 579 ν(Fe–O).
(C) SA solid: ~3300–2400br ν(OH); 1655 $\nu(C=O)_{dimer}$; 1610, 1579, 1482, 1465 $\nu(CC)_{ar}$; 1443 $\nu(CC)_{ar}$ or $\beta(COH)_{O=C-OH}$; 1383w $\beta(COH)_{Ar-OH}$; 1324 $\nu(CC)_{ar}$ or $\nu(CO)_{O=C-OH}$; 1292 $\nu(CO)_{O=C-OH}$ + β(CH); 1247 $\nu(CO)_{Ar-OH}$ or ν(CH); 1209 β(COH) or $\nu(CO)_{Ar-OH}$; 1188 ν(CH); 1155, 1089, 1030 β(CH); 867 $\beta_s(COO^-)$ or γ(CH); 659 γ(C=O).

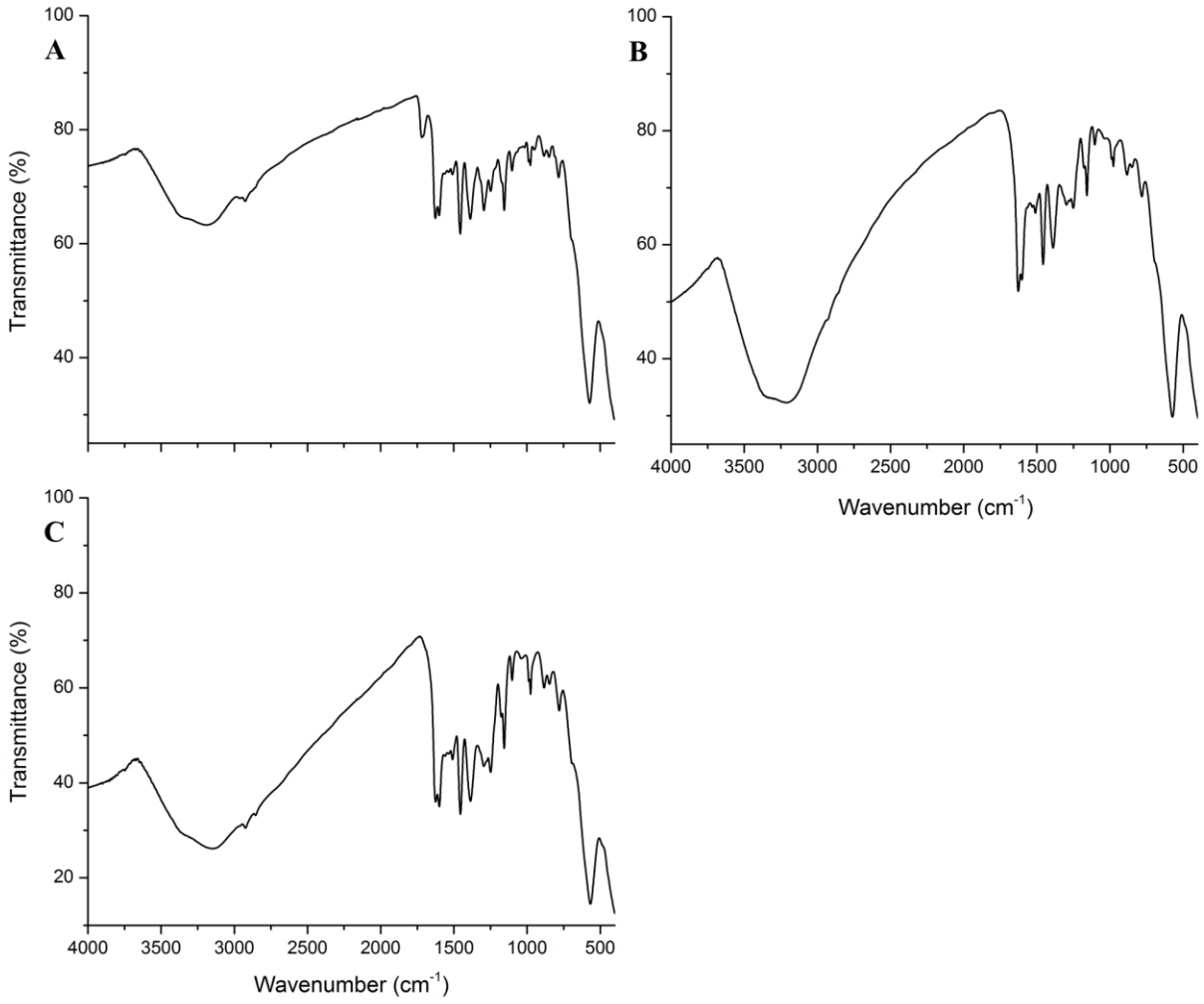

Figure S13. FTIR spectra of (A) IONP-2,4-DHBA (HCl preparation), with select bands as follows (in cm^{-1}): 3194br ν(OH); 2926 $\nu_{as}(CH_2)$; 1719 ν(C=O); 1627 $\nu(C{=}O)_{dimer}$ + $\nu(CC)_{ar}$; 1599 $\nu_{as}(COO^-)$; 1534w, 1509, 1456 $\nu(CC)_{ar}$; 1387 $\nu_s(COO^-)$, 1294 $\nu(CO)_{O=C-OH}$ + β(CH); 1248 $\nu(CO)_{Ar-OH,\ 2\text{-}OH}$; 1155, 1102 β(CH); 571 ν(Fe–O).
(B) IONP-2,4-DHBA (HCl, 6 washes acetone): 3213br ν(OH); 1627 $\nu(C{=}O)_{dimer}$ + $\nu(CC)_{ar}$; 1602 $\nu_{as}(COO^-)$; 1530w, 1509, 1457 $\nu(CC)_{ar}$; 1389 $\nu_s(COO^-)$, 1298, 1276vw $\nu(CO)_{O=C-OH}$ + β(CH); 1251, 1276vw $\nu(CO)_{Ar-OH,\ 2\text{-}OH}$; 1177, 1158, 1104 β(CH); 572 ν(Fe–O).
(C) IONP-2,4-DHBA (DI water): 3152br ν(OH); 2924 $\nu_{as}(CH_2)$; 2855 $\nu_s(CH_2)$; 1625 $\nu(C{=}O)_{dimer}$ + $\nu(CC)_{ar}$; 1600 $\nu_{as}(COO^-)$; 1520w, 1508, 1455 $\nu(CC)_{ar}$; 1386 $\nu_s(COO^-)$, 1295 $\nu(CO)_{O=C-OH}$ + β(CH); 1249 $\nu(CO)_{Ar-OH,\ 2\text{-}OH}$; 1157, 1102 β(CH); 567 ν(Fe–O).

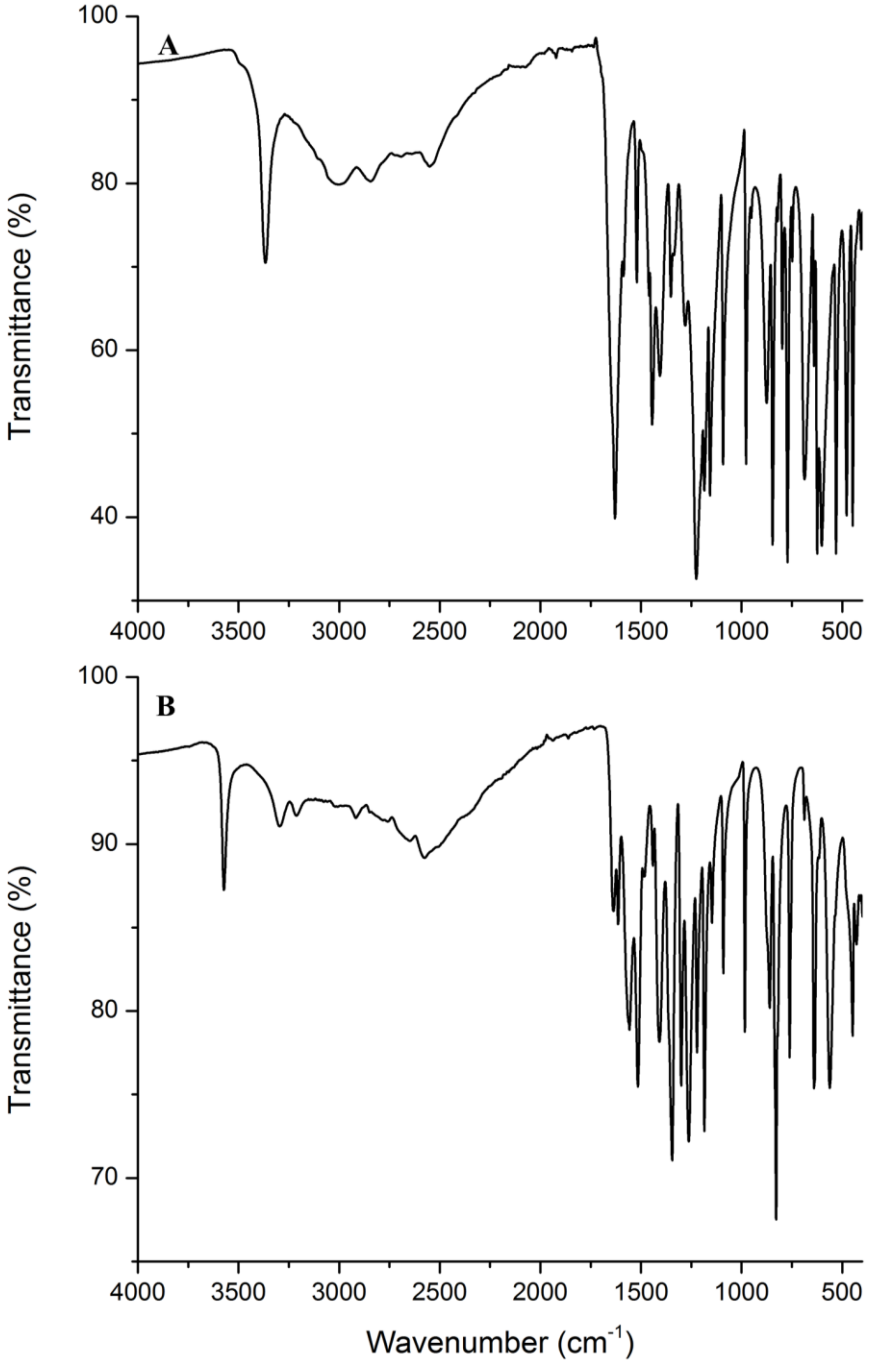

Figure S14. FTIR spectra of (A) 2,4-DHBA solid, with key bands as follows (in cm^{-1}): ~3300–2550br ν(OH); 1629br $\nu(C{=}O)_{dimer}$ + $\nu(CC)_{ar}$; 1521, 1444, 1352 $\nu(CC)_{ar}$; 1406 β(COH); 1280 $\nu(CO)_{O=C-OH}$ + β(CH); 1225 $\nu(CO)_{Ar-OH,\ 4\text{-}OH}$; 1157, 1092 β(CH); 748 β(C=O).
(B) sodium salt of 2,4-DHBA (Na-2,4-DHB): ~3575–2570br ν(OH); 1636 $\nu(C{=}O)_{dimer}$ + $\nu(CC)_{ar}$; 1557 $\nu_{as}(COO^-)$; 1515, 1441, 1345 $\nu(CC)_{ar}$; 1408 β(COH); 1483 or 1325 $\nu_s(COO^-)$; 1300 $\nu(CO)_{O=C-OH}$ + β(CH); 1263 $\nu(CO)_{Ar-OH,\ 2\text{-}OH}$; 1222 $\nu(CO)_{Ar-OH,\ 4\text{-}OH}$; 1147, 1091 β(CH); 761 β(C=O).

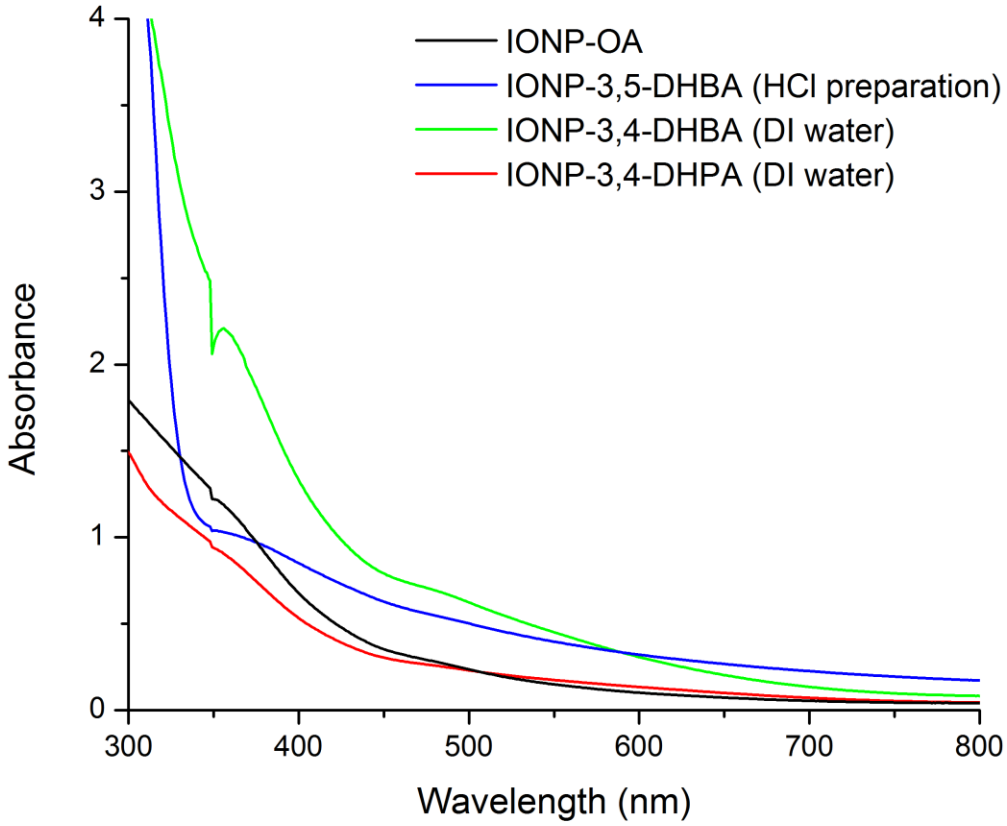

Figure S15. UV–visible solution spectra comparing the absorption profile of IONP-OA against various ligand exchanged nanoparticles.

Table S13. Modified Nanoparticle Purification Parameters for Some Samples Prepared for UV–Visible (UV–Vis) Spectroscopy and Electrokinetic Measurements

Nanoparticle	Reaction mixture volume (mL)	1st wash	2nd wash	Solvent used for resuspension
UV–Vis Spectroscopy				
IONP-OA	N/A	N/A	N/A	hexane
IONP-3,4-DHPA	4	3 x 2 mL hexane	3 x 2 mL methanol	3 mL 0.2 M Tris buffer pH 9.22
IONP-3,4-DHBA	3	3 x 1.5 mL hexane	3 x 1.5 mL methanol	2.25 mL 0.2 M Tris buffer pH 9.22
IONP-3,5-DHBA	2	3 x 1 mL hexane	3 x 1 mL (1:1) isopropanol/methanol	0.4 mL 20 mM NaOAc[a] buffer pH 4.94
Electrokinetic Measurements				
IONP-3,4-DHPA	4	3 x 2 mL hexane	3 x 2 mL methanol	1.65 mL 0.2 M Tris buffer pH 9.21
IONP-3,4-DHBA	4	3 x 2 mL hexane	3 x 2 mL methanol	1.7 mL 0.2 M Tris buffer pH 9.21

[a]NaOAc = sodium acetate.

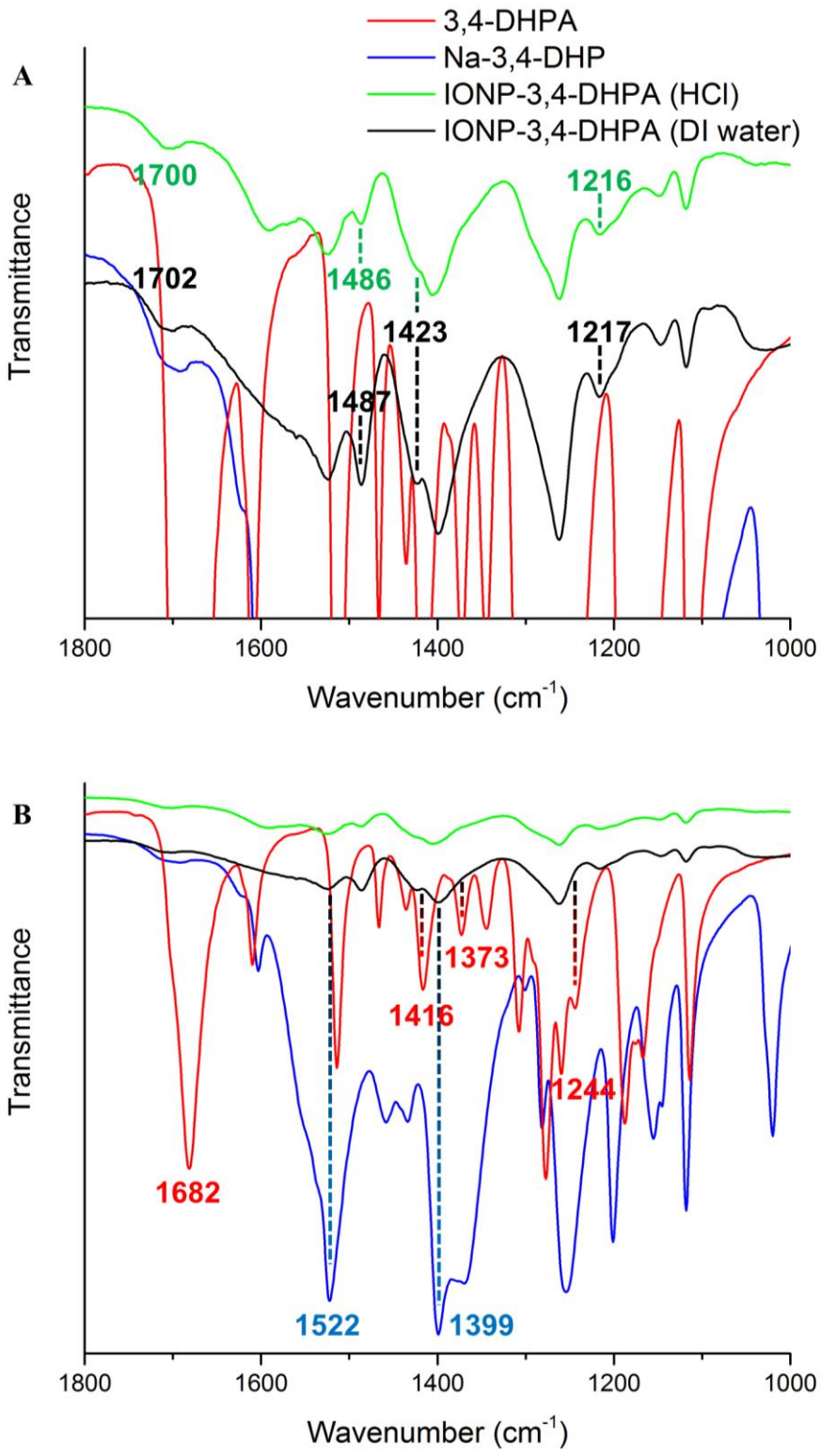

Figure S16. Comparison of bands relevant to ligand binding in the FTIR spectra of (A, B) 3,4-DHPA and against their corresponding sodium salt and functionalized nanoparticles. For some bands, dotted lines are added to guide the eye. Scale has been adjusted in (A) to view the nanoparticle spectra more closely.

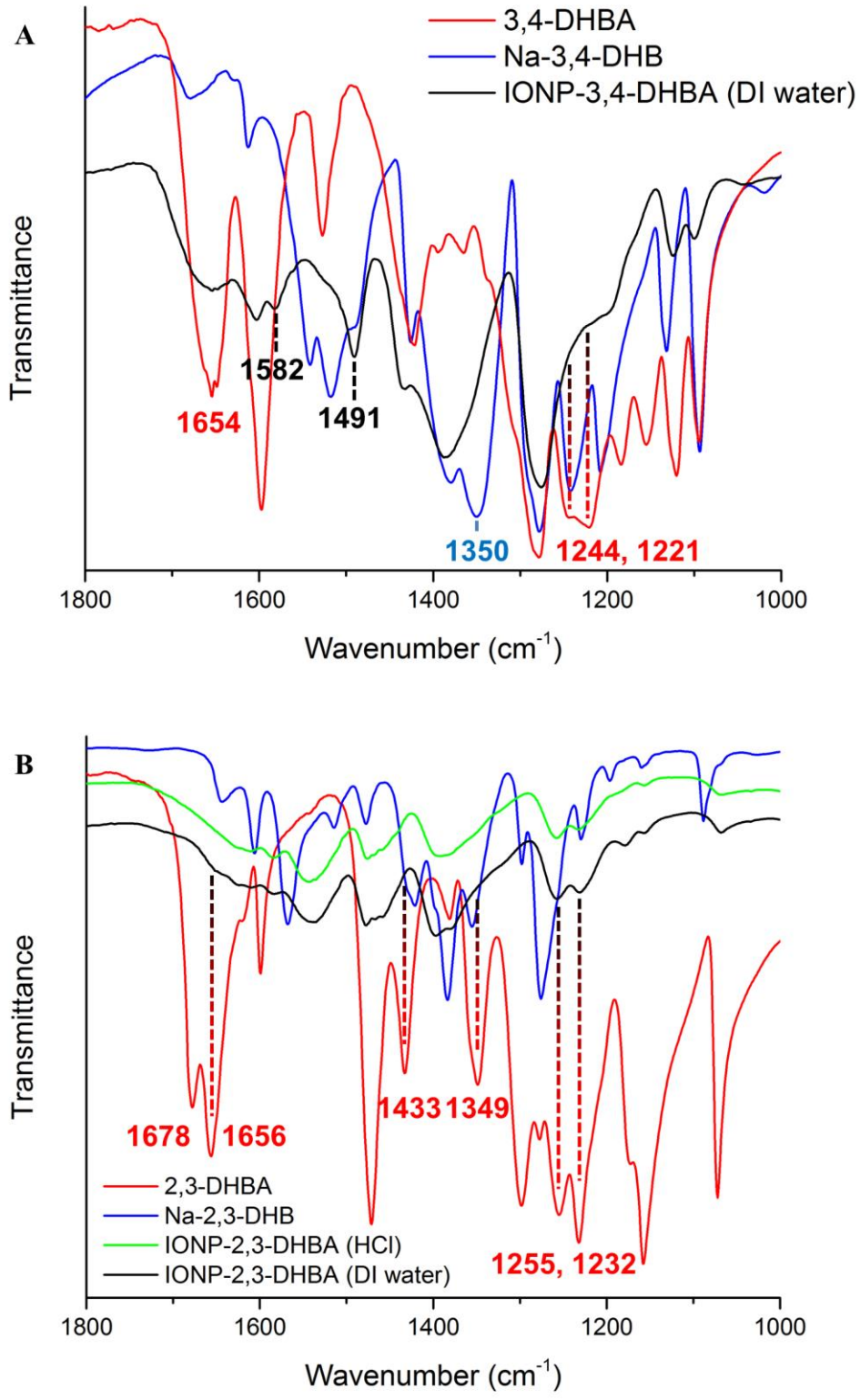

Figure S17. Comparison of bands relevant to ligand binding in the FTIR spectra of (A) 3,4-DHBA and (B) 2,3-DHBA against their corresponding sodium salt and functionalized nanoparticles. For some bands, dotted lines are added to guide the eye.

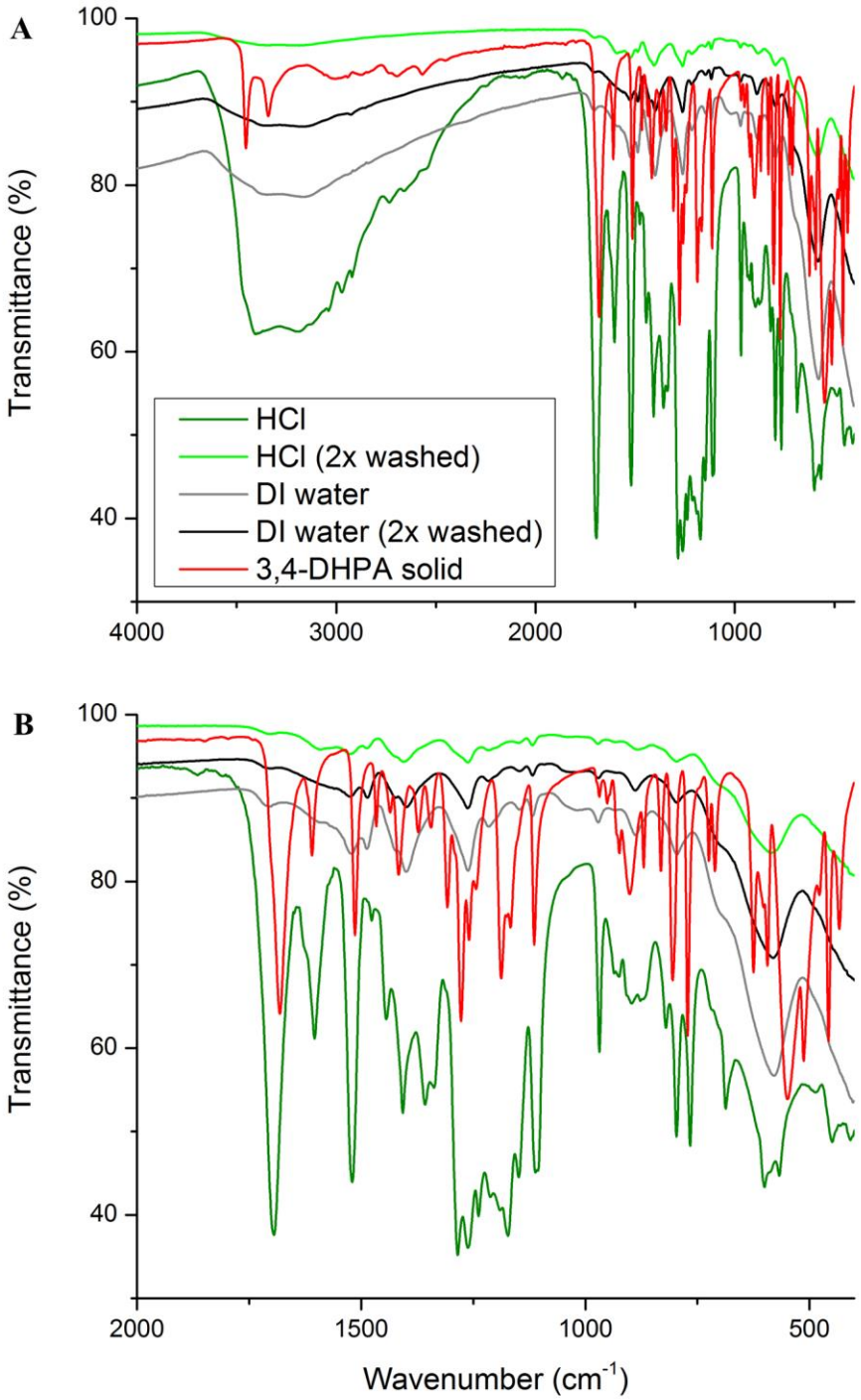

Figure S18. FTIR spectra comparing the IONP-3,4-DHPA HCl added, HCl (2x washed), DI water added, and DI water (2x washed) preparations with 3,4-DHPA solid showing the removal of excess 3,4-DHPA, and other reaction by-products, with continued purification by washing with acetone.

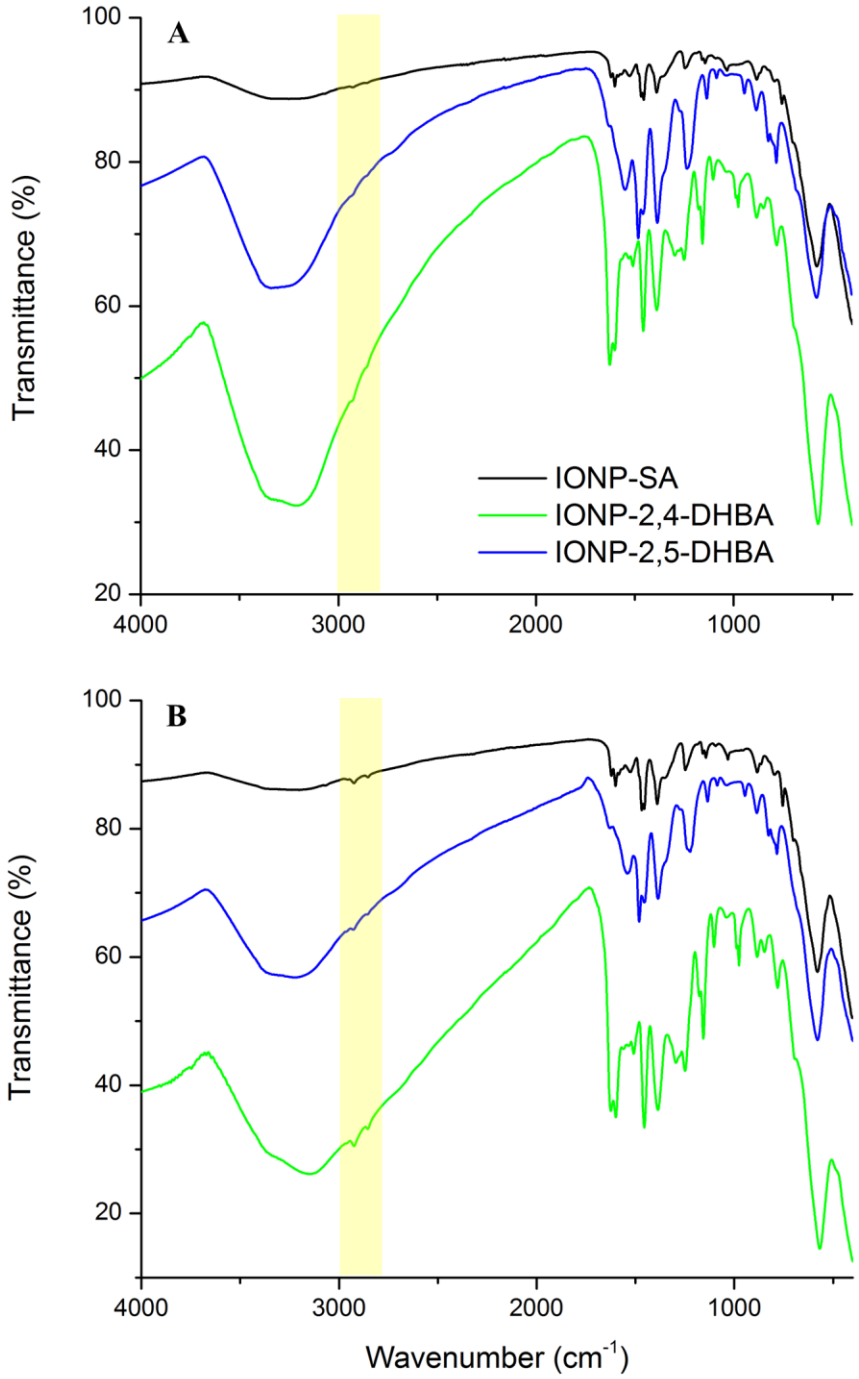

Figure S19. FTIR spectra of IONP-SA, IONP-2,4-DHBA, and IONP-2,5-DHBA synthesized under (A) HCl added or (B) DI water added conditions. Methylene vibrations ($\nu_{as,s}(CH_2)$) are highlighted in yellow.

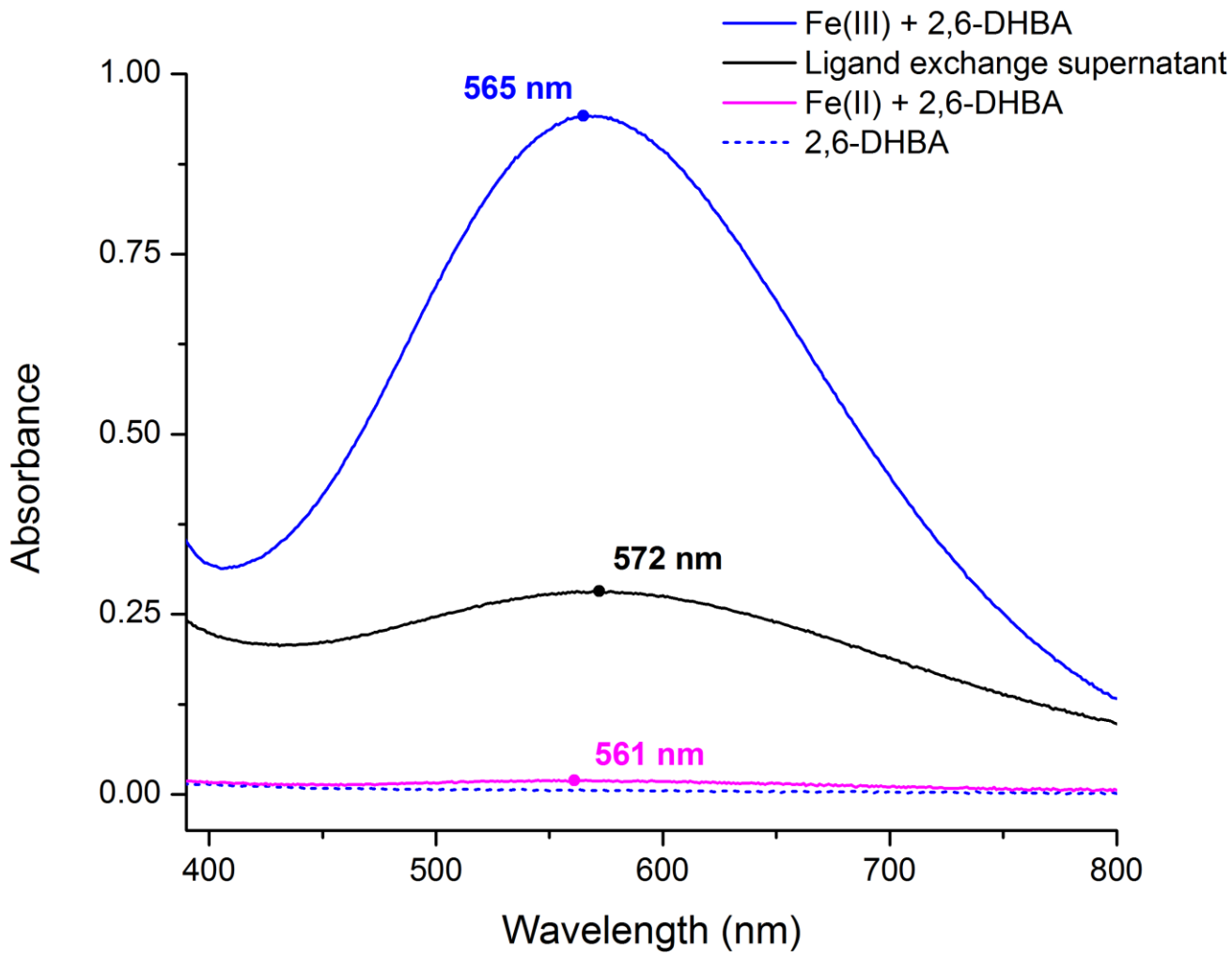

Figure S20. Solution spectra from 390–800 nm of the ligand exchange supernatant recovered from the attempted ligand exchange reaction of 2,6-DHBA with IONP-OA (HCl added conditions), prepared complexes of Fe(II) or Fe(III) and 2,6-DHBA, and a control where only 2,6-DHBA (in 1:1 methanol/0.1 M HCl(aq)) is present. Peak maxima in the visible range are indicated.

Table S14. Ligand Exchange Supernatant Colors and Visible Spectra Maxima.

Ligand	Color	λ_{max}, supernatant (nm)	λ_{max}, Fe(III)–ligand complex (nm)
2,6-DHBA	Indigo	572	565 (This work)
2,3-DHBA	Indigo	578	575[41]
SA	Purple-violet	525	520–530[42]
2,5-DHBA	Green-blue	589, 362	590[43]

Additional Analysis

FTIR Analysis of the Iron Oxide Nanoparticle Core Structure. According to the literature, Fe_3O_4 (magnetite) has no distinct spectral features in the IR above 600 cm^{-1},[6a, 6b, 44] with bulk magnetite presenting an Fe–O band at 570 cm^{-1}.[5] In contrast, γ-Fe_2O_3 (maghemite) presents a series of bands above 600 cm^{-1}.[6a, 45] These differences in spectral features for Fe_3O_4 versus Fe_2O_3 allow us to assign the strong *ν*(Fe–O) vibration at 591 and 580 cm^{-1} for IONP-OA to that of Fe_3O_4. The vibration is slightly blue-shifted from the measurement of Fe_3O_4 in bulk, likely due to the consequence of under-coordination of surface atoms (compared to bulk) of nanosized iron oxide leading to an increase in the force constant for Fe–O.[46]

The broad *ν*(Fe–O) band does extend above 600 cm^{-1} with an additional broad shoulder around 690 cm^{-1} for both preparations of IONP-OA. Weak absorbances are also visible at around 700 cm^{-1} in the spectra of IONP-3,4-DHPA, IONP-2,3-DHBA, IONP-3,4-DHBA, IONP-3,5-DHBA, IONP-2,5-DHBA (~681/686 cm^{-1} for HCl/DI water), and IONP-2,4-DHBA (~695/692 cm^{-1} for HCl/DI water). These weak shoulders around 690 cm^{-1} may point to an oxidized shell of iron oxide, maghemite, around the magnetite nanoparticle core.[6a, 45, 47] Both batches of prepared IONP-OA had similar IR spectra except for the position of the Fe–O stretch. The shift in *ν*(Fe–O) to higher wavenumbers for the first batch of IONP-OA may be a result of oxidation over time during storage at -20 °C (FTIR spectra of IONP-OA (Batch 1) was obtained 4 months after nanoparticle synthesis), or increased oxidation during the initial preparation and purification of the nanoparticles.

References

1. Nagesha, D. K.; Plouffe, B. D.; Phan, M.; Lewis, L. H.; Sridhar, S.; Murthy, S. K. Functionalization-induced improvement in magnetic properties of Fe_3O_4 nanoparticles for biomedical applications. *J. Appl. Phys.* **2009,** *105* (7), 07B317.
2. Korpany, K. V.; Mottillo, C.; Bachelder, J.; Cross, S. N.; Dong, P.; Trudel, S.; Friščić, T.; Blum, A. S. One-step ligand exchange and switching from hydrophobic to water-stable hydrophilic superparamagnetic iron oxide nanoparticles by mechanochemical milling. *Chem. Commun.* **2016,** *52* (14), 3054–3057.
3. Larkin, P. *Infrared and Raman Spectroscopy: Principles and Spectral Interpretation*; Elsevier: Waltham, MA, 2011.
4. Lambert, J. B.; Shurvell, H. F.; Lightner, D. A.; Cooks, R. G. *Introduction to Organic Spectroscopy*; Macmillan: New York, 1987; pp 133-245.
5. (a) Liese, H. C. An infrared absorption analysis of magnetite. *Am. Mineral.* **1967,** *52*, 1198–1205; (b) Waldron, R. D. Infrared Spectra of Ferrites. *Phys. Rev.* **1955,** *99* (6), 1727–1735.
6. (a) Hu, L.; Percheron, A.; Chaumont, D.; Brachais, C. H. Microwave-assisted one-step hydrothermal synthesis of pure iron oxide nanoparticles: magnetite, maghemite and hematite. *J. Sol-Gel Sci. Technol.* **2011,** *60* (2), 198–205; (b) Iwasaki, T.; Sato, N.; Nakamura, H.; Watano, S. Mechanochemical formation of superparamagnetic magnetite nanoparticles from ferrihydrite over a wide range of pH environments. *Mater. Chem. Phys.* **2013,** *140* (2–3), 596–601; (c) Cai, W.; Wan, J. Facile synthesis of superparamagnetic magnetite nanoparticles in liquid polyols. *J. Colloid Interface Sci.* **2007,** *305* (2), 366–370; (d) Sundrarajan, M.; Ramalakshmi, M. Novel Cubic Magnetite Nanoparticle Synthesis Using Room Temperature Ionic Liquid. *E-Journal of Chemistry* **2012,** *9* (3), 1070–1076; (e) Wang, C. Y.; Hong, J. M.; Chen, G.; Zhang, Y.; Gu, N. Facile method to synthesize oleic acid-capped magnetite nanoparticles. *Chin. Chem. Lett.* **2010,** *21* (2), 179–182.
7. (a) Söderlind, F.; Pedersen, H.; Petoral, R. M., Jr.; Käll, P. O.; Uvdal, K. Synthesis and characterisation of Gd_2O_3 nanocrystals functionalised by organic acids. *J. Colloid Interface Sci.* **2005,** *288* (1), 140–148; (b) Wu, N.; Fu, L.; Su, M.; Aslam, M.; Wong, K. C.; Dravid, V. P. Interaction of Fatty Acid Monolayers with Cobalt Nanoparticles. *Nano Lett.* **2004,** *4* (2), 383–386; (c) Willis, A. L.; Turro, N. J.; O'Brien, S. Spectroscopic Characterization of the Surface of Iron Oxide Nanocrystals. *Chem. Mater.* **2005,** *17* (24), 5970–5975.
8. Gong, W. Q.; Parentich, A.; Little, L. H.; Warren, L. J. Adsorption of oleate on apatite studied by diffuse reflectance infrared Fourier transform spectroscopy. *Langmuir* **1992,** *8* (1), 118–124.
9. (a) Bloemen, M.; Brullot, W.; Luong, T. T.; Geukens, N.; Gils, A.; Verbiest, T. Improved functionalization of oleic acid-coated iron oxide nanoparticles for biomedical applications. *J. Nanopart. Res.* **2012,** *14* (9), 1100; (b) Roonasi, P.; Yang, X.; Holmgren, A. Competition between sodium oleate and sodium silicate for a silicate/oleate modified magnetite surface studied by in situ ATR-FTIR spectroscopy. *J. Colloid Interface Sci.* **2010,** *343* (2), 546–552; (c) Hofmann, A.; Thierbach, S.; Semisch, A.; Hartwig, A.; Taupitz, M.; Rühl, E.; Graf, C. Highly monodisperse water-dispersable iron oxide nanoparticles for biomedical applications. *J. Mater. Chem.* **2010,** *20* (36), 7842–7853.
10. (a) Zhang, L.; He, R.; Gu, H. C. Oleic acid coating on the monodisperse magnetite nanoparticles. *Appl. Surf. Sci.* **2006,** *253* (5), 2611–2617; (b) Mahdavi, M.; Ahmad, M. B.; Haron, M. J.; Namvar, F.; Nadi, B.; Rahman, M. Z.; Amin, J. Synthesis, Surface Modification

and Characterisation of Biocompatible Magnetic Iron Oxide Nanoparticles for Biomedical Applications. *Molecules* **2013,** *18* (7), 7533–7548.
11. Fang, C.; Bhattarai, N.; Sun, C.; Zhang, M. Functionalized Nanoparticles with Long-Term Stability in Biological Media. *Small* **2009,** *5* (14), 1637–1641.
12. Bronstein, L. M.; Huang, X.; Retrum, J.; Schmucker, A.; Pink, M.; Stein, B. D.; Dragnea, B. Influence of Iron Oleate Complex Structure on Iron Oxide Nanoparticle Formation. *Chem. Mater.* **2007,** *19* (15), 3624–3632.
13. Kalinowska, M.; Świsłocka, R.; Borawska, M.; Piekut, J.; Lewandowski, W. Spectroscopic (FT-IR, FT-Raman, UV) and microbiological studies of di-substituted benzoates of alkali metals. *Spectrochim. Acta, Part A* **2008,** *70* (1), 126–135.
14. Láng, L.; Varsányi, G. *Assignments for vibrational spectra of seven hundred benzene derivatives*; New York, Wiley: New York, 1974.
15. Colthup, N. B., Daly, L. H.; Wiberly, S. E. *Introduction to infrared and Raman spectroscopy,* 2nd ed.; Academic Press: New York, NY, 1975.
16. Pretsch, E.; Clerc, T.; Seibl, J.; Simon, W. *Tables of Spectral Data for Structure Determination of Organic Compounds,* 2nd ed.; Springer-Verlag: Berlin, Germany, 1989.
17. (a) Park, S. K.; Lee, N. S.; Lee, S. H. Vibrational Analysis of Dopamine Neutral Base based on Density Functional Force Field. *Bull. Korean Chem. Soc.* **2000,** *21* (10), 1035–1038; (b) Gunasekaran, S.; Kumar, R. T.; Ponnusamy, S. Vibrational spectra and normal coordinate analysis of adrenaline and dopamine. *Indian J. Pure Appl. Phys.* **2007,** *45* (11), 884–892.
18. Basti, H.; Ben Tahar, L.; Smiri, L. S.; Herbst, F.; Vaulay, M. J.; Chau, F.; Ammar, S.; Benderbous, S. Catechol derivatives-coated Fe_3O_4 and γ-Fe_2O_3 nanoparticles as potential MRI contrast agents. *J. Colloid Interface Sci.* **2010,** *341* (2), 248–254.
19. Amstad, E.; Gehring, A. U.; Fischer, H.; Nagaiyanallur, V. V.; Hähner, G.; Textor, M.; Reimhult, E. Influence of Electronegative Substituents on the Binding Affinity of Catechol-Derived Anchors to Fe_3O_4 Nanoparticles. *J. Phys. Chem. C* **2011,** *115* (3), 683–691.
20. Suzuki, H.; Nagasaka, M.; Sugiura, M.; Noguchi, T. Fourier Transform Infrared Spectrum of the Secondary Quinone Electron Acceptor Q_B in Photosystem II. *Biochemistry* **2005,** *44* (34), 11323–11328.
21. Anandhan, K.; Kumar, R. T. Density functional theory calculation on dopamine. *J. Chem. Pharm. Sci.* **2011,** *4* (2), 73–78.
22. Saikia, N.; Sarma, J.; Borah, J. M.; Mahiuddin, S. Adsorption of 3,4-dihydroxybenzoic acid onto hematite surface in aqueous medium: Importance of position of phenolic -OH groups and understanding of the same using catechol as an auxiliary model. *J. Colloid Interface Sci.* **2013,** *398*, 227–233.
23. Janković, I. A.; Šaponjić, Z. V.; Čomor, M. I.; Nedeljlković, J. M. Surface Modification of Colloidal TiO_2 Nanoparticles with Bidentate Benzene Derivatives. *J. Phys. Chem. C* **2009,** *113* (29), 12645–12652.
24. (a) Guan, X. H.; Shang, C.; Chen, G. H. ATR-FTIR investigation of the role of phenolic groups in the interaction of some NOM model compounds with aluminum hydroxide. *Chemosphere* **2006,** *65* (11), 2074–2081; (b) Borah, J. M.; Sarma, J.; Mahiuddin, S. Adsorption comparison at the α-alumina/water interface: 3,4-Dihydroxybenzoic acid vs. catechol. *Colloids Surf., A* **2011,** *387* (1–3), 50–56.
25. Kamariotaki, M.; Karaliota, A.; Stabaki, D.; Bakas, T.; Papaefthymiou, V.; Perlepes, S. P.; Hadjiliadis, N. Coordination complexes of iron(III) with 3-hydroxy-2(1H)-pyridinone, 2,3-

dihydroxybenzoic acid and 3,4-dihydroxybenzoic acid: preparation and characterization in the solid state. *Transition Met. Chem.* **1994,** *19* (2), 241–247.
26. Sun, Y.; Wang, Y.; Zhitomirsky, I. Dispersing agents for electrophoretic deposition of TiO_2 and TiO_2–carbon nanotube composites. *Colloids Surf., A* **2013,** *418*, 131–138.
27. Litos, C.; Terzis, A.; Raptopoulou, C.; Rontoyianni, A.; Karaliota, A. Polynuclear oxomolybdenum(VI) complexes of dihydroxybenzoic acids: Synthesis, spectroscopic and structure characterization of a tetranuclear catecholato-type coordinated 2,3-dihydroxybenzoate and a novel tridentate salicylato-type coordinated 2,5-dihydroxybenzoate trinuclear complex. *Polyhedron* **2006,** *25* (6), 1337–1347.
28. Jadrijević-Mladar Takač, M.; Vikić Topić, D. FT-IR and NMR spectroscopic studies of salicylic acid derivatives. II. Comparison of 2-hydroxy- and 2,4- and 2,5-dihydroxy derivatives. *Acta Pharm.* **2004,** *54* (3), 177–191.
29. (a) Hanna, K.; Quilès, F. Surface Complexation of 2,5-Dihydroxybenzoic Acid (Gentisic Acid) at the Nanosized Hematite-Water Interface: An ATR-FTIR Study and Modeling Approach. *Langmuir* **2011,** *27* (6), 2492–2500; (b) Regulska, E.; Kalinowska, M.; Wojtulewski, S.; Korczak, A.; Sienkiewicz-Gromiuk, J.; Rzączyńska, Z.; Świsłocka, R.; Lewandowski, W. Theoretical (in B3LYP/6-3111++G** level), spectroscopic (FT-IR, FT-Raman) and thermogravimetric studies of gentisic acid and sodium, copper(II) and cadmium(II) gentisates. *Spectrochim. Acta, Part A* **2014,** *132*, 713–725.
30. Krishnakumar, V.; Surumbarkuzhali, N. Analysis of structure and vibrational spectra of 2,5-dihydroxybenzoicacid based on density functional theory calculations. *J. Raman Spectrosc.* **2010,** *41* (4), 473–478.
31. Ibrahim, M.; Nada, A.; Kamal, D. E. Density functional theory and FTIR spectroscopic study of carboxyl group. *Indian J. Pure Appl. Phys.* **2005,** *43* (12), 911–917.
32. Volovšek, V.; Colombo, L.; Furić, K. Vibrational Spectrum and Normal Coordinate Calculations of the Salicylic Acid Molecule. *J. Raman Spectrosc.* **1983,** *14* (5), 347–352.
33. Humbert, B.; Alnot, M.; Quilès, F. Infrared and Raman spectroscopical studies of salicylic and salicylate derivatives in aqueous solution. *Spectrochim. Acta, Part A* **1998,** *54* (3), 465–476.
34. Biber, M. V.; Stumm, W. An In-Situ ATR-FTIR Study: The Surface Coordination of Salicylic Acid on Aluminum and Iron(III) Oxides. *Environ. Sci. Technol.* **1994,** *28* (5), 763–768.
35. Yost, E. C.; Tejedor-Tejedor, M. I.; Anderson, M. A. In Situ CIR-FTIR Characterization of Salicylate Complexes at the Goethite/Aqueous Solution Interface. *Environ. Sci. Technol.* **1990,** *24* (6), 822–828.
36. Guan, X. H.; Chen, G. H.; Shang, C. ATR-FTIR and XPS study on the structure of complexes formed upon the adsorption of simple organic acids on aluminum hydroxide. *J. Environ. Sci.-China* **2007,** *19* (4), 438–443.
37. (a) Dobson, K. D.; McQuillan, A. J. In situ infrared spectroscopic analysis of the adsorption of aromatic carboxylic acids to TiO_2, ZrO_2, Al_2O_3, and Ta_2O_5 from aqueous solutions. *Spectrochim. Acta, Part A* **2000,** *56* (3), 557–565; (b) Tunesi, S.; Anderson, M. A. Surface Effects in Photochemistry: An in Situ Cylindrical Internal Reflection-Fourier Transform Infrared Investigation of the Effect of Ring Substituents on Chemisorption onto TiO_2 Ceramic Membranes. *Langmuir* **1992,** *8* (2), 487–495.
38. Lewandowski, W.; Dasiewicz, B.; Koczoń, P.; Skierski, J.; Dobrosz-Teperek, K.; Świsłocka, R.; Fuks, L.; Priebe, W.; Mazurek, A. P. Vibrational study of alkaline metal nicotinates, benzoates and salicylates. *J. Mol. Struct.* **2002,** *604* (2–3), 189-193.

39. Tao, Y.; Han, L.; Han, Y.; Liu, Z. A combined experimental and theoretical analysis on molecular structure and vibrational spectra of 2,4-dihydroxybenzoic acid. *Spectrochim. Acta, Part A* **2015,** *137*, 1078–1085.
40. Tejedor-Tejedor, M. I.; Yost, E. C.; Anderson, M. A. Characterization of Benzoic and Phenolic Complexes at the Goethite/Aqueous Solution Interface Using Cylindrical Internal Reflection Fourier Transform Infrared Spectroscopy. Part 1. Methodology. *Langmuir* **1990,** *6* (5), 979–987.
41. Xu, J.; Jordan, R. B. Equilibrium and Kinetic Studies of the Complexing of Iron(III) by 1,2-Dihydroxybenzene Derivatives. *Inorg. Chem.* **1988,** *27* (8), 1502–1507.
42. (a) Ernst, Z. L.; Menashi, J. Complex Formation between the Fe^{3+} ion and some Substituted Phenols. Part 1.-Spectrophotometric Determination of the Stability Constant of Ferric Salicylate. *Trans. Faraday Soc.* **1963,** *59*, 1794–1802; (b) Ou, X.; Wang, C.; Zhang, F. J.; Quan, X.; Ma, Y.; Liu, H. Complexation of iron by salicylic acid and its effect on atrazine photodegradation in aqueous solution. *Front. Environ. Sci. Eng. China* **2010,** *4* (2), 157–163; (c) Mehlig, J. P. Colorimetric Determination of Iron with Salicyclic Acid. *Ind. Eng. Chem., Anal. Ed.* **1938,** *10* (3), 136–139.
43. Porwal, S. K.; Furia, E.; Harris, M. E.; Viswanathan, R.; Devireddy, L. Synthetic, potentiometric and spectroscopic studies of chelation between Fe(III) and 2,5-DHBA supports salicylate-mode of siderophore binding interactions. *J. Inorg. Biochem.* **2015,** *145*, 1–10.
44. Namduri, H.; Nasrazadani, S. Quantitative analysis of iron oxides using Fourier transform infrared spectrophotometry. *Corros. Sci.* **2008,** *50* (9), 2493–2497.
45. Klotz, M.; Ayral, A.; Guizard, C.; Menager, C.; Cabuil, V. Silica Coating on Colloidal Maghemite Particles. *J. Colloid Interface Sci.* **1999,** *220* (2), 357–361.
46. Ma, M.; Zhang, Y.; Yu, W.; Shen, H.; Zhang, H.; Gu, N. Preparation and characterization of magnetite nanoparticles coated by amino silane. *Colloids Surf. A* **2003,** *212* (2–3), 219–226.
47. Daou, T. J.; Grenèche, J. M.; Pourroy, G.; Buathong, S.; Derory, A.; Ulhaq-Bouillet, C.; Donnio, B.; Guillon, D.; Begin-Colin, S. Coupling Agent Effect on Magnetic Properties of Functionalized Magnetite-Based Nanoparticles. *Chem. Mater.* **2008,** *20* (18), 5869–5875.